NASA TECHNICAL TRANSLATION NASA TM 75161

CONCEPTS FOR THE DESIGN OF A COMPLETELY ACTIVE HELICOPTER ISOLATION SYSTEM USING OUTPUT VECTOR FEEDBACK

G. Schulz

Translation of "Konzepte zur Auslegung eines vollaktiven Hubschrauber-Schwingungs Isolations Systems mittels Ausgangsvektorrückführung", DEUTSCHE Forschungs- und Versuchsanstalt fuer Luft- und Raumfahrt, Oberpfaffenhofen (West Germany) Report DLR-DB-552-76/12, Sept. 1976, 63 pages

NATIONAL AERONAUTICS AND SPACE ADMINISTRATION
WASHINGTON, D. C. 20546 OCTOBER 1977

STANDARD TITLE PAGE

1. Report No. NASA TM 75161	2. Government Accession No.	3. Recipient's Catalog No.
4. Title and Subtitle CONCEPTS FOR THE DESIGN OF A COMPLETELY ACTIVE HELICOPTER ISOLATION SYSTEM USING OUTPUT VECTOR FEEDBACK		5. Report Date October 1977 6. Performing Organization Code
7. Author(s) G. Schulz		8. Performing Organization Report No. 10. Work Unit No.
9. Performing Organization Name and Address SCITRAN Box 5456 Santa Barbara, CA 93108		11. Contract or Grant No. NASw-2791 13. Type of Report and Period Covered Translation
12. Sponsoring Agency Name and Address National Aeronautics and Space Administration Washington, D.C. 20546		14. Sponsoring Agency Code

15. Supplementary Notes
Translation of "Konzepte zur Auslegung eines vollaktiven Hubschrauber-Schwingungs Isolations Systems mittels Ausgangsvektorruckfuhrung", DEUTSCHE Forschungs- und Versuchsanstalt fuer Luft- und Raumfahrt, Oberpfaffenhofen (West Germany), Report DLR-DB-552-76/12, Sept. 1976, 63 pages.

16. Abstract
Concepts using the theory of output vector feedback (a few measured quantities) for controller design are worked out for the completely active oscillation isolation function for helicopters. These controller concepts are tested with various versions of the BO 105 helicopter and their performance is demonstrated. A compensation of the vibrational excitations from the rotor, harmonics of the number of blades, are compensated for. There is also a fast and automatic trim function for maneuvers.

17. Key Words (Selected by Author(s))	18. Distribution Statement
	Unclassified - Unlimited

19. Security Classif. (of this report)	20. Security Classif. (of this page)	21. No. of Pages	22.
Unclassified	Unclassified	68	

ABSTRACT

Concepts using the theory of output vector feedback (a few measured quantities) for controller design are worked out for the completely active oscillation isolation function for helicopters. These controller concepts are tested with various versions of the BO 105 helicopter and their performance is demonstrated. A compensation of the vibrational excitations from the rotor, harmonics of the number of blades, are compensated for. There is also a fast and automatic trim function for maneuvers.

DFVLR, Flight Mechanics and Flight Control Division. Institute for Flight Systems Dynamics Control System Division.

Oberpfaffenhofen, September 15, 1976

Research Director: Dr. F. Thomas
Institute Director: Dr.-Ing. J. Ackermann
Division Chief: R. Sharma, Professional Engineer

TABLE OF CONTENTS

/ 1*

* Numbers in margin indicate pagination in original foreign text.

NOTATION LIST

m_R	Mass of the rotor-gear unit
m_Z	(generalized) mass of the airframe
k_Z, d_Z	(generalized) spring and damping constants of the body
$P_R(t)$	Vertical excitation force (in the fixed body system)
z_Z, z_o	Absolute deflection of the center of mass of the body
Δz	Relative deflection between rotor gear unit and body
$P_A(t)$	Actuator force
z_o	Actuator deflection
$\overline{\Delta z} = \frac{\Delta z}{z_o}$	Normalized deflection of Δz
$\overline{z}_z = \frac{z_z}{z_o}$	Normalized deflection of z_Z
$m_{ges} = m_R + m_z$	Helicopter mass
$\overline{P}_R = \frac{P_R}{m_{ges} \cdot g}$	Normalized excitation force P_R
Ω	Rotation frequency
$\frac{1}{\delta} = \frac{g \cdot m_{ges}}{z_o \cdot m_R \cdot \Omega^2}$	Normalized perturbation amplification
$M = \frac{m_R}{m_R + m_z}$	Mass ratio
$\frac{1}{\gamma} = \frac{A \cdot p_S}{z_o \cdot m_R \cdot \Omega^2}$	Normalized actuator amplification
p_S	Supply pressure of actuator
$\psi = \Omega \cdot t$	Rotor rotation angle
$\overline{\omega}_z = \frac{1}{\Omega}\sqrt{\frac{k_z}{m_z}}$	Normalized eigenfrequency of body structure

Δp	Normalized control pressure difference
u	Normalized control variable
C_{sv}	Amplification factor
$\underline{x}$	State vector of systems
A	Dynamics matrix of system
$\underline{b}$	Actuator vector of system
$\underline{b}_S$	Actuator vector of system perturbation
C	Measurement matrix of system
$\underline{y}$	Measurement vector of system
$z_z^{*''}$	Approximate body acceleration
T_ψ	Time constant when measuring body acceleration
d_Δ, k_Δ	(generalized) spring and damping constant of the intermediate support
F_{Tz}	Isolation force
$K_1^*, K_2^*, K_3^*, K_4^*, K^*$	Control matrices
$\underline{x}_r$	State vector of controller
$\underline{y}^*$	Extended output vector of systems
$\underline{z}$	State vector of perturbation model
F	Dynamics matrix
G_u, G_y	Input matrices
H	Output matrix
$\hat{\underline{x}}$	Estimated values of the state system
$\hat{\underline{x}}_S$	Estimated values of perturbation state
K_1, K_2	Matrices of Riccati feedback

} of observer

/ 3

C^*	Transformation matrix for extending the output vector $\underline{y}$
Δp	Pressure difference of actuator
J_i	Parts of the quality criterion
α_i	Weighting coefficients of quality criterion
Ω, R	Weighting matrices
N	Dynamics matrix of the Notch isolator.

/4

CONCEPTS FOR THE DESIGN OF A COMPLETELY ACTIVE HELICOPTER ISOLATION SYSTEM USING OUTPUT VECTOR FEEDBACK*

G. Schulz

1. INTRODUCTION

Within the framework of the ASIS ZKP program, the DFVLR, I 1552 in collaboration with the Firm MBB-UD, performed theoretical investigations for the design of an active oscillation isolation system (ASIS) for the BO 105 helicopter. Also controllers were designed for insulating the isolations for modes of low order. Using controllable hydraulic servoelements, these controllers have the purpose of isolating the rotor-gear unit from the airframe of the helicopter, and the following tasks are satisfied by them over the entire operational range:

i) Suppression or strong reduction of perturbing airframe vibrations which are harmonics of the blade number

ii) Limitation of the static or quasi-static relative motions between the rotor-gear unit and the airframe using an automatic trim device.

* DFVLR (German Research and Test Facility for Aviation and Spaceflight) Internal Report 552-76/12.

Since exactly known discrete frequencies occur in helicopter vibrations, it is not necessary to provide wideband isolation of the airframe. For successful oscillation isolation, it is only necessary to suppress or attenuate the low blade-harmonic (that is $4\,\Omega$ to maximum $12\,\Omega$) perturbation frequencies.

Previous investigations of the Firm MBB [1] assumed that the differential equations (state variables) together with all the derivatives used in the computer model of the airframe/rotor-gear unit are measured, and are used as input variables for the controller. With this assumption, the resulting controllers are extremely simple and easy to calculate, because they do not have any eigen dynamics. However, in the case of the helicopter not all state variables are available and therefore in this report we make the realistic assumption for the controller design that only a few output quantities are available as measured variables. The controller must then be designed using a method of output vector feedback and then has eigen dynamics.

In this report we design the controller with output vector feedback according to two different methods. The designs are compared with respect to satisfying the design criteria, susceptibility to perturbations and the possibility of building them. We also discuss its use for higher order systems and when helicopter airframe mode shapes are considered.

2. HELICOPTER COMPUTER MODELS FOR VERTICAL OSCILLATION ISOLATION

/5

2.1. Computer models for velocity feedback of the cell (Model 1)

In [1], the differential equations for the completely active oscillation insulation system with pressure servocontrol are given. When these differential equations are established, the simple helicopter computer model of Figure 1 is assumed. Here the rotor-gear unit and the airframe are idealized by means of two discrete point masses which are connected together through the active servoelement , which is a force generator. There is an additional soft support of the airframe through a special spring-damper element, which simulates the elastic airframe behavior for each mode shape. The vertical excitation which is transferred from the rotor to the airframe is introduced as an external perturbation force P_R.

The two mass system of Figure 1 leads to the following differential equation system

$$\Delta\bar{z}'' = 2\cdot\bar{\omega}_z\cdot\zeta_z\cdot\bar{z}_z' + \bar{\omega}_z^2\cdot\bar{z}_z + \frac{1}{(1-M)\gamma}\cdot\Delta\bar{p} + \frac{1}{\delta}\cdot\bar{P}_R \qquad (1)$$

$$\bar{z}_z'' = -2\cdot\bar{\omega}_z\cdot\zeta_z\cdot\bar{z}_z' - \bar{\omega}_z^2\cdot\bar{z}_z - \frac{M}{(1-M)\gamma}\cdot\Delta\bar{p} \qquad (2)$$

where

$$\Delta\bar{p} = c_{SV}\cdot u \qquad (3)$$

The derivatives $' \triangleq \frac{d}{d\bar{\psi}}$ are derivatives with respect to the angle $\bar{\psi}$.

The deflection of the rotor-gear unit $\Delta\bar{z}$ and the velocity of the airframe deflection $\bar{z}_z$, are measured which then are

available as input variables for the controller. The control variable u is the output quantity of the controller.

The state representation for Model I therefore has the following appearance

$$\underline{x}' = A\,\underline{x} + \underline{b} \cdot u + \underline{b}_S \cdot v \tag{4}$$

$$\underline{y} = C\,\underline{x} \tag{5}$$

with the matrices and vectors

$$A = \begin{bmatrix} 0 & 1 & 0 & 0 \\ 0 & 0 & 1 & 0 \\ 0 & \bar{\omega}_z^2 & 0 & 2\zeta\bar{\omega}_z \\ 0 & -\bar{\omega}_z^2 & 0 & -2\zeta\bar{\omega}_z \end{bmatrix} \qquad \underline{b} = \begin{bmatrix} 0 \\ 0 \\ \frac{C_{SV}}{(1-M)\gamma} \\ \frac{M \cdot C_{SV}}{(1-M)\gamma} \end{bmatrix} \tag{6}$$

$$\underline{b}_S^T = [\,0 \quad 0 \quad \frac{1}{\delta} \quad 0\,]$$

$$\underline{x}^T = [\,\Delta\bar{z} \quad \bar{z}_z \quad \Delta\bar{z}' \quad \bar{z}_z'\,]$$

$$C = \begin{bmatrix} 1 & 0 & 0 & 0 \\ 0 & 0 & 0 & 1 \end{bmatrix}$$

and $v = \bar{P}_R$

/ 6

The numerical values for the matrices A, $\underline{b}$, $\underline{b}_S$ are

$$A = \begin{bmatrix} 0 & 0 & 0 & 0 \\ 0 & 0 & 1 & 0 \\ 0 & 11.57 & 0 & 0.068 \\ 0 & -11.57 & 0 & -0.068 \end{bmatrix} \qquad b = \begin{bmatrix} 0 \\ 0 \\ 8.15 \\ -1.24 \end{bmatrix} \qquad b_S = \begin{bmatrix} 0 \\ 0 \\ 6.53 \\ 0 \end{bmatrix} \tag{7}$$

The block diagram of the system with the controller is shown in Figure 2.

2.2. Computer model for the acceleration feedback of the airframe (Model II)

For the computer Model II with acceleration feedback, again the helicopter excitation model of Figure 1 is used. This means that the same differential equations (1) and (2) result for the system as for Model I. In contrast to Model I, we now assume that the airframe acceleration is measured z''_z and fed back. Because of the measurement technique (exact acceleration measuring devices), this acceleration feedback is preferred over velocity feedback. In order to avoid that then a system results which could jump (same degree of the numerator and denominator polynomial), a delay unit (time constant T_ψ) is introduced for measuring the acceleration. This delay is represented by the following additional differential equation

$$(\bar{z}''_z)' = -\frac{1}{T_\psi}\,\bar{z}''_z + \frac{1}{T_\psi}\cdot z''_z \quad . \tag{8}$$

If in Equation (8) we now replace z''_z by Equation (2), then we find the following state model

$$\underline{x}' = A\,\underline{x} + \underline{b}\,u + \underline{b}_S\,v \tag{4}$$

$$\underline{y} = C\,\underline{x} \tag{5}$$

with the matrices and vectors

$$A = \begin{bmatrix} 0 & 1 & 0 & 0 & 0 \\ 0 & 0 & 1 & 0 & 0 \\ 0 & \bar{\omega}_z^2 & 0 & 2\zeta\bar{\omega}_z & 0 \\ 0 & -\bar{\omega}_z^2 & 0 & -2\zeta\bar{\omega}_z & 0 \\ 0 & -\frac{\bar{\omega}_z^2}{T_\psi} & 0 & -\frac{2\zeta\bar{\omega}_z}{T_\psi} & -\frac{1}{T_\psi} \end{bmatrix} \qquad \underline{b} = \begin{bmatrix} 0 \\ 0 \\ \frac{C_{SV}}{(1-M)\,\gamma} \\ \frac{C_{SV}\cdot H}{(1-M)\,\gamma} \\ \frac{C_{SV}\cdot H}{(1-M)\,\gamma\cdot T_\psi} \end{bmatrix} \tag{9}$$

$$\underline{b}_S^T = [\,0 \quad 0 \quad \frac{1}{\delta} \quad 0 \quad 0\,]$$

$$\underline{x}^T = [\,\Delta\bar{z} \quad \bar{z}_z \quad \Delta\bar{z}' \quad \bar{z}_z' \quad z^{**}\,]$$

$$C = \begin{bmatrix} 1 & 0 & 0 & 0 & 0 \\ 0 & 0 & 0 & 0 & 1 \end{bmatrix}$$

and $v = P_R$.

The numerical values for the matrices A, $\underline{b}$, $\underline{b}_S$ are

$$A = \begin{bmatrix} 0 & 1 & 0 & 0 & 0 \\ 0 & 0 & 1 & 0 & 0 \\ 0 & 11.57 & 0 & 0.068 & 0 \\ 0 & -11.57 & 0 & -0.068 & 0 \\ 0 & -11.57\cdot 10^3 & 0 & -0.068\cdot 10^3 & -10^3 \end{bmatrix} \qquad \underline{b} = \begin{bmatrix} 0 \\ 0 \\ 8.15 \\ -1.24 \\ 8.15\cdot 10^3 \end{bmatrix} \qquad (10)$$

$$\underline{b}_S^T = [\,0 \quad 0 \quad 6.53 \quad 0 \quad 0\,] \,.$$

2.3. Computer model for feedback of the actuator pressure difference (Model III)

In order to determine the computer Model III for feeding back the actuator pressure difference, an intermediate support between the rotor gear mass and the mass of the helicopter airframe is assumed (see Figure 3). Based on the experience with Model I [1], we here only assume a feedback of the relative deflection $\Delta\bar{z}$ of the rotor gear unit and the pressure difference $\Delta\bar{p}$ in the pressure servo. In this way the deflections of u are attenuated as fast as possible, because the helicopter airframe is only excited to perform vibrations through the coupling of the servo $(+P_{A'} - P_A)$ because there is no soft intermediate support.

Figure 3 shows the free system without ground support (k_z, d_z). In [2] a differential equation system is given for it which contains only the relative deflection $\Delta\bar{z}$ and the pressure difference $\Delta\bar{p}$ of the pressure servo with the derivatives as state variables. The acceleration $\bar{z}_o''$ of the airframe is determined from a linear combination of the state variables through the force $\bar{F}_{Tz}$ which acts on the airframe or the rotor-gear unit:

$$\bar{F}_{Tz} = \frac{m_z \cdot \Omega^2 \cdot \delta_o}{\theta_{Ges}} \cdot \bar{z}_o'' \qquad (11)$$

$$\bar{F}_{Tz} = 0.34485\ \Delta\bar{z} - 4.27090\ \Delta\bar{p} + 0.02299\ \Delta\bar{z}' \quad \text{(isolation condition)} \qquad (12)$$

The state vector contains the following elements / 8

$$\underline{x}^T = [\ \Delta\bar{z} \quad \Delta\bar{p} \quad \Delta\dot{\bar{z}}' \quad \Delta\dot{\bar{p}}'\ ] \qquad (13)$$

The numerical values of the matrices of the state model according to Equations (4) and (5)

$$\underline{x}' = A\,\underline{x} + \underline{b}\,u + \underline{b}_S\,\bar{v} \qquad (4)$$

$$\underline{y} = C\,\underline{x} \qquad (5)$$

are

$$A = \begin{bmatrix} 0 & 0 & 1 & 0 \\ 0 & 0 & 0 & 1 \\ -2.655 & 32.88152 & -0.177 & 0 \\ 0 & -805.33179 & -204.1257 & -28.37837 \end{bmatrix} \qquad \underline{b} = \begin{bmatrix} 0 \\ 0 \\ 0 \\ 805.33179 \end{bmatrix} \qquad (14)$$

$$\underline{b}_S^T = [\ 0 \quad 0 \quad 6.52455 \quad 0\ ]$$

where $v = P_R$ and

$$C = \begin{bmatrix} 1 & 0 & 0 & 0 \\ 0 & 1 & 0 & 0 \end{bmatrix}$$

3. METHODS OF DESIGN OF CONTROLLERS FOR OUTPUT VECTOR FEEDBACK

In Sections 3.1 and 3.2 we give two methods of controller design which allow the system to be controlled without knowledge of the total state vector $\underline{x}$. These concepts are tailored to the boundary conditions found in practice, where there is only a limited number of elements of the state vector available, which can be measured, and only these are available as input signals for the controller. Using this method, the number of measurement units can be considerably reduced or, if the mode eigen oscillations of the airframe are taken into account, it becomes possible to control the helicopter without measuring all components of the eigen oscillation mode.

3.1. Design of a dynamic compensator with additional notch-isolator (Controller I)

Starting with the investigations of [3], a numerical method of controller design with output vector feedback is developed in [4] and [5]. A separate consideration of the design criteria mentioned in the introduction is then possible:

i) Suppression or strong attenuation of perturbing airframe vibrations which are harmonic with the blade number

II) Limitation of the static or quasi-static relative motions between the rotor-gear unit and the airframe with an automatic trim device

Both criteria were separately weighted during the design and this led to a single controller.

During the optimization, the generalized quality criterion is minimized which consists of a weighted sum of three individual criteria

$$J = \alpha_1 J_1 + \alpha_2 J_2 + \alpha_3 J_3 \qquad (15)$$

where

$$J_m = \int_0^\infty \{ y_m^T Q_m y_m + \underline{u}^T R_m \underline{u} \} dt$$

For m = 1 the deviations are weighted when there is a disturbance (Figure 4a). For m = 2 the deviations when there is a nominal value jump u is weighted (Figure 4b). For m = 3 the transient behavior of the system after an initial deflection y_o (Figure 4c) is weighted.

Therefore the design criterion i) is considered using the quality criterion J_1 and the design criterion ii) is considered with the quality criterion J_2. The additional weighting of the transient behavior (quality criterion J_3) is prevented by slow transient processes.

A Notch isolator is installed in the controller for detecting the perturbation. Figure 5 shows the structure of controller I. One can see three main components (meaning of the dashed line - see Section 4.4):

i) On the top the integration of output y_1 with subsequent amplification k_1. /10

ii) In the center the proportional feedback of output $\underline{y}$.

iii) Below the dynamic part of the control with the dynamics matrix K_1^* which also contains the daynamic matrix N of the Notch isolator.

The matrices K_i^* are summarized as follows in the matrix K^*

$$K^* = \begin{bmatrix} K_1^* & K_2^* \\ K_3^* & K_4^* \end{bmatrix} \tag{16}$$

The notch isolator is contained in K_4^* as follows:

$$K_4^* = \begin{bmatrix} K_{4R}^* & 0 \\ 0 & N \end{bmatrix} \tag{17}$$

The optimization program now calculates the free parameters of the K* matrix and the additional integral feedback parameter k_1 using minimization of the quality criterion J.

3.2. Design of a state and perturbation observer with subsequent Riccati feedback (Controller II).

For this observer design [6] with subsequent Riccati feedback, the complete state of the system and the perturbation are reconstructed from the available measurements (relative deflection $\Delta\bar{z}$ of the rotor-gear unit and the airframe velocity $\bar{z}_Z$). In this way no notch isolator is required in the controller. The information on the perturbation is given by the observer (perturbation observer) (Figure 6).

Using the Riccati design [7] a constant feedback matrix $K_c = [K_1, J_2]$ is designed using a minimization of a quadratic quality criterion according to Figure 4a)

$$J = \int_0^\infty (\underline{x}^T Q_R \underline{x} + \underline{u}^T R_R \underline{u})\, dt \tag{15}$$

where

$$\underline{x}^T \triangleq [\underline{x}^T \quad \underline{x}_S^T].$$

Figure 7 shows the resulting controller. First the single and double integral of the first component $y_1 = \Delta z$ of the output is formed and the vector $\underline{y}$ is extended to form the new vector $\underline{y}^*$ (Figure 6c).

The matrices F, G_u, G_y, H and T (where $z = T \cdot x$) are calculated in the observer design. The matrices $K_c = [K_1, K_2]$ follow from the Riccati design. The following conversion then gives

$$R_c = [R_1 \mid R_2] = [K_1 \mid K_2] \cdot \left[\frac{C}{T}\right]^{-1}$$

where $H = \left[\frac{C}{T}\right]^{-1}$ (Figure 6b). / 11

$$K_R = \left[\begin{array}{c|c} R_1 & R_2 \\ \hline G_y + G_u \cdot R_1 & F + G_u \cdot R_2 \end{array}\right] \qquad (18)$$

and the intermediate numerical values are calculated.

In contrast to controller I, the design criterion (i) is systematically covered (according to Figure 4a). By proper selection of the weighting matrices Ω_R and R_R, the design criterion ii) (see introduction) is approximately satisfied.

4. COMPLETELY ACTIVE OSCILLATION ISOLATION OF THE HELICOPTER BO 105 - CALCULATED RESULTS AND SYSTEMS ANALYSIS IN THE TIME AND FREQUENCY RANGE /12

In this section we will discuss the performance of the controller discussed in Section 3 and its use for oscillation isolation in the helicopter BO 105. The following design goals must be met - discussed in Sections 4.1 and 4.3.

α) Oscillation isolation (Criterion i)) must be obtained with the normalization of the variables

1. $u < 1/3$
2. $\bar{z}'_z$ bzw. $\bar{z}''_z \to 0$
3. $\Delta\bar{z} < 0.2$.

β) In order to limit the quasistatic relative motions Criterion ii)) (maneuver case) we must have

1. $\Delta\bar{z} < 0.2$.

In Section 4.4 we apply the following design criteria with different normalization of the variables

α) 1. $u < 0.6$
2. $\Delta\bar{z} < 0.2$
3. $\Delta\bar{p} < 0.6$

β) 1. $\Delta\bar{z} < 0.2$.

4.1. Design of the dynamic compensators (Controller I) for velocity feedback (Model I)

The optimization of the controller results in the following controller matrix K* (see Section 3.1)

$$K^* = \left[\begin{array}{cc|cccc} -21.87 & -3.22 & 0 & 1 & 0 & 1 \\ 401.49 & 25.21 & 0 & -26.46 & 0 & 0 \\ 256.88 & 12.88 & 1 & -15.23 & 0 & 0 \\ 0 & 6.67 & 0 & 0 & 0 & -16 \\ 0 & -0.2 & 0 & 0 & 1 & 0 \end{array}\right] \qquad (19)$$

and the additional feedback

$$K_1 = -3.33$$

of the integral through $\Delta\bar{z}$. /13

The time variations of the state and controller variables for the perturbation compensation are given in Figures 8 to 13.

Figure 8: Variation of perturbation.

Figures 9 - 12: Transient behavior of airframe. The airframe settles down after about 1.5 rotor revolutions (Figures 10 and 11).

The actuator variable u then goes to zero (Figure 13).

Figures 15 to 18 show the trim behavior of the system after a 2.5 g maneuver given in Figure 14 (1 - 2.5 g in 0.5 sec).

The maximum deflection of $\Delta\bar{z}$ remains below 0.2. We have $|\Delta\bar{z}|_{MAX} \approx 0.02$ (Figure 16).

The design criteria given above are therefore satisfied.

The error sensitivity if there is a mismatch of the notch isolator is shown in the following. Figures 19 - 23 show the time variation when the perturbation frequency is changed by - 3%. Figures 24 - 28 show the time variations when the perturbation

frequency is changed by + 3%. The helicopter airframe no longer settles down.

The Bode diagrams of the perturbation transfer functions of the control system are given in Figures 29 - 31. Clearly the effectiveness of the Notch isolator can be seen in Figure 31 for $\omega = 4$.

4.2: Design of the dynamic compensater (Controller I) for acceleration feedbakc (Model II)

Optimization of the controller gives the following controller matrix K

$$K^* = \left[\begin{array}{cc|cccc} -8.06 & -0.34 & 0 & 1 & 0 & 1 \\ \hline 52.32 & -7.04 & 0 & -11.43 & 0 & 0 \\ 50.66 & 1.66 & 1 & -8.90 & 0 & 0 \\ 0 & 0.26 & 0 & 0 & 0 & -16 \\ 0 & -0.20 & 0 & 0 & 1 & 0 \end{array}\right] \qquad (20)$$

and the additional feedback

$$k_1 = -1.39$$

of the integral through $\Delta\bar{z}$.

The time variations of the state and controller variables for the perturbation variable compensation are given in Figures 32 to 38.

Figure 32: Perturbation history.

Figures 32 to 37: Transient behavior of the airframe. The airframe settles down after about 2 rotor revolutions.

The controlled variable u goes to zero (Figure 38).

Figures 40 to 45 show the trim behavior of the system for a 2.5 g maneuver of Figure 39.

The maximum deflection in $\Delta\bar{z}$ remains below 0.2, and we have $|\Delta\bar{z}|_{MAX} \approx 0.04$ (Figure 41). /14

Therefore the design criteria given above are satisfied.

The Bode diagrams of the perturbation transfer functions of the control system are given in Figure 46 - 48.

4.3. Design of the observer with Riccati feedback (Controller II) for velocity feedback (Model I)

Optimization of the controller gives the following controller matrix K_R (see Section 3.2)

$$K_R = \left[\begin{array}{cccc|cccc} -79.41 & -11.92 & -30.36 & 56.30 & 51.79 & -253.90 & 3.21 & -25.40 \\ -7.39 & 0.74 & -2.21 & 2.95 & 0.47 & -21.82 & 0.34 & -2.68 \\ -15.82 & -0.92 & -2.90 & 7.09 & 3.36 & -45.98 & 0.52 & -4.10 \\ 340.17 & 51.74 & 132.28 & -238.74 & -220.52 & 1081.16 & -15.68 & 110.17 \\ -27.14 & -0.27 & -10.91 & 25.08 & 20.31 & -99.57 & -0.74 & -11.97 \end{array}\right] \quad (21)$$

The time variations of the state and control variables for the perturbation compensation are given in Figures 49 to 54.

Figure 49: Variation of perturbation

Figures 50 - 53: Transient behavior of airframe. The airframe settles down after about 1 1/4 rotor revolutions.

The controlled variable u goes to zero (Figure 54).

Figures 56 to 60 show the trim behavior of the system for a 2.5 g maneuver of Figure 55.

The maximum deflection $\Delta\bar{z}$ just reaches the allowable limit of 0.2. An additional reduction in the deflection $\Delta\bar{z}$ leads to a controller which does not completely compensate for the vibrational disturbance. Residual vibrations then remain.

The air sensitivity for a perturbation frequency $\omega_s^* = \omega_s (1 + 3\%)$ increased by 3% is shown in Figures 61 to 65. It is shown in Figures 66 to 70 for $\omega_s^* = \omega_s (1 - 3\%)$. The relevant quantities, the airframe deflection $\bar{z}_z$ and the airframe velocity $\bar{z}'_z$, have deflections which are about 10 times smaller than when controller I is used (Figures 19 to 28). This perturbation observer is less sensitive to mismatches than the Notch isolator.

The Bode diagrams of the perturbation transfer functions (Figures 71 to 73) confirm this insensitivity regarding the mismatch as Figure 73 shows. The gap at $\omega = 4$ is clearly wider than in Figure 31 or Figure 48.

4.4. Design of the dynamic compensator (Controller I) for feedback of temperature difference of the actuator (Model III). /15

The optimization of the controller results in the following controller matrix K^*.

$$K^* = \left[\begin{array}{cc|cccc} -5.04 & -1.95 & 0 & 1 & 0 & 1 \\ \hline 2.33 & 15.93 & 0 & -3.83 & 0 & 0 \\ 28.54 & -.29 & 1 & -7.36 & 0 & 0 \\ 1.02 & -16.99 & 0 & 0 & 0 & -16 \\ -0.20 & -.72 & 0 & 0 & 1 & 0 \end{array}\right] \qquad (22)$$

and the additional feedback $k_1 = -0.41$ of the integral through $\Delta\bar{z}$.

In contrast to the basic Controller I (Figure 5) the integral $\int \Delta\bar{z}\, d\psi$ is also introduced into the dynamic part of the controller (see dashed line). For this purpose, the matrix K_3^* is extended to

$$K_3^* = \left[\begin{array}{ccc} 2.33 & 15.93 & 1.56 \\ 28.54 & -.29 & 3.36 \\ 1.04 & -16.99 & 0. \\ -0.20 & -.72 & 0 \end{array}\right] \qquad (23)$$

The time variations of the state and control variables for the perturbation variable compensation are given in Figures 74 to 80. Since Controller I does not simulate the state, the Notch isolator is also not excited according to the isolation condition (Equation 12). The airframe acceleration $\bar{z}_o''$ is proportional to $\bar{F}_{Tz}$ and does not go completely to zero.

Figures 82 to 86 show the trim behavior of the system after a 2.5 g maneuver according to Figure 81. The relative deflection remains within the permissible limit $|\Delta\bar{z}|_{MAX} \approx 0.03$.

The Bode diagrams of perturbation transfer functions are given in Figures 87 to 89.

4.5. Comparison of results regarding satisfaction of the design criteria, the perturbation sensitivity of the design, the computer calculation requirement for the design and the feasibility

Investigations in this chapter have shown that the method of output vector feedback for controller design can be applied to the problem of oscillation isolation of helicopters using a few measured quantities. The system motions remain within the design limits. Two different methods of controller design were investigated, a dynamic compensator (Controller I) and an observer

with Riccati feedback (Controller II). /16

The system motions during the transient processes for perturbation compensation are clearly smaller for Controller II than for Controller I. For the Controller I in Figure 11, we have $|\bar{z}_z|_{MAX} \approx 0.02$ and for Controller II in Figure 52 $|\bar{z}_z|_{MAX} \approx 0.004$. The duration of the transient process is about 1 - 1.5 rotor revolutions in both cases. On the other hand, the maximum deflection $\Delta\bar{z}$ of the rotor-gear unit for Controller I is clearly smaller ($|\Delta\bar{z}|_{MAX} \approx 0.02$, Figure 16) than for Controller II ($|\Delta\bar{z}|_{MAX} \approx 0.2$, Figure 57). For Controller II, we reached the design limit at the relative deflection $\Delta\bar{z}$. For Controller I the amplitude of $\bar{z}_z$ can still be decreased to offset $\Delta\bar{z}$. One can also expect that the error sensitivity will decrease if there is a mismatch of the Notch isolator (Figures 19 to 28 compared with Figures 61 to 70, also the Bode diagrams, Figure 31, compared with Figure 73).

The systematics of the design of Controller I allows one to consider several criteria but the computation times are large (about 30 to 50 minutes of CPU time). On the other hand, the Controller II only requires small computation times (about 1 - 3 minutes of CPU time) for a computer run.

In addition, the Controller I has a reduced number of parameters (about 10-15) and is easier to build than Controller II (about 40 parameters). Controller II is more complex. The simple integral over $\Delta\bar{z}$ is not sufficient to satisfy the design goals. The relative deflection $\Delta\bar{z}$ must be integrated twice in order to reach the design goal $\int\int (|\Delta\bar{z}| \leq 0.2)$.

Sections 4.2 and 4.4 discuss the Controller I for two additional helicopter models (II and III), and its effectiveness is demonstrated.

We were able to show that tested and effective controller concepts with output vector feedback are available which allow a completely active oscillation isolation system for a helicopter. These controllers do not require the complete state vector of the system as input variables, to eliminate disturbance or for guaranteeing trimming during maneuvers. They only require the output vector, which has a low order (a few measurement terms). This means that these controllers can also be used when eigen oscillation modes of the airframe are considered, without measuring the corresponding oscillation mode and their derivatives. We must only guarantee that these oscillation modes can be observed with a single measurement variable.

5. SUMMARY AND OUTLOOK /17

In this report we discussed concepts for designing a completely active helicopter isolation system using output vector feedback. Three different dynamic models of the helicopter including rotor-gear unit were introduced. Two high performance methods for controller design using output vector feedback were applied to the helicopter models mentioned above, a dynamic compensator and an observer with Riccati feedback. The two design criteria for perturbation compensation with vibration excitation which is harmonic with the blade number as well as trim behavior for a 2.5 g maneuver were maintained with the controller design. These controllers do not require the knowledge of the entire state vector for satisfying the design goals. Therefore, their structure is very well suited for controlling higher order models, i.e., helicopter models including modes of the airframe.

6. REFERENCES

1. Strehlow, H., Hagemann, W., Theoretical Concept of a Completely Active Helicopter Oscillation Isolation System. TN-D123-18/75, Messerschmitt-Bolkow-Blohm GmbH, Rotary Aircraft Branch.

2. Strehlow, H., Written communication of August 25, 1976.

3. Anderson, B. D. O., Moore, J. B., Linear Optimal Control Prentice Hall, Inc., Englewood Cliffs, N. J., 1971.

4. Kreisselmeier, G., Quadratic Synthesis with Partial State Vector Feedback. Lecture for the course "Linear Optimum Control" of the Carl Crantz society, October, 1975.

5. Kreisselmeier, G., Use of Quadratic Synthesis with Partial State Vector Feedback for Controller Design. Lecture for the course "Linear Optimum Control" of the Carl Crantz Society, October, 1975.

6. Luenberger, D. G. An Introduction to Observers, IEEE-Trans. on Automatic Control, Vol. AC-16, No. 6, December, 1971.

7. Bryson, A. E., Ho, Y. C., Applied Optimal Control, Blaisdell Publ. Comp., Waltham, Mass. 1969.

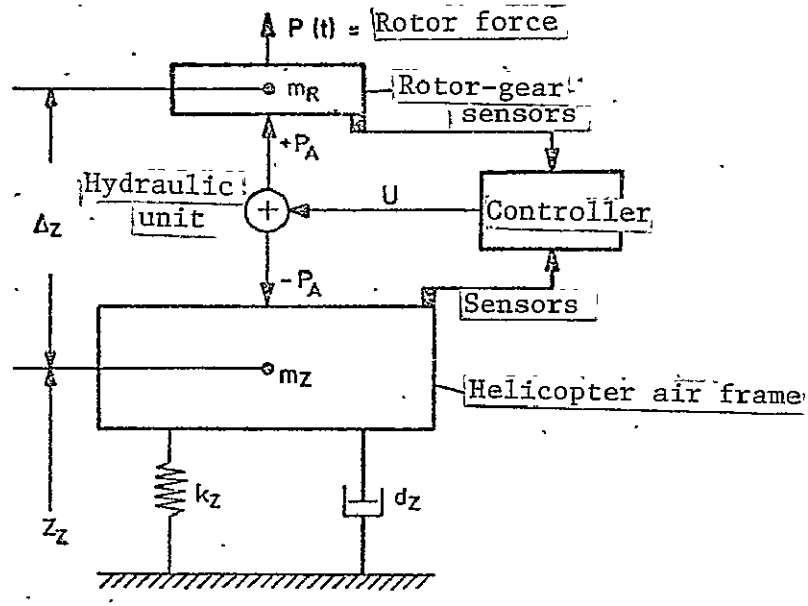

Figure 1. Helicopter model 1 for a completely active oscillation isolation system.

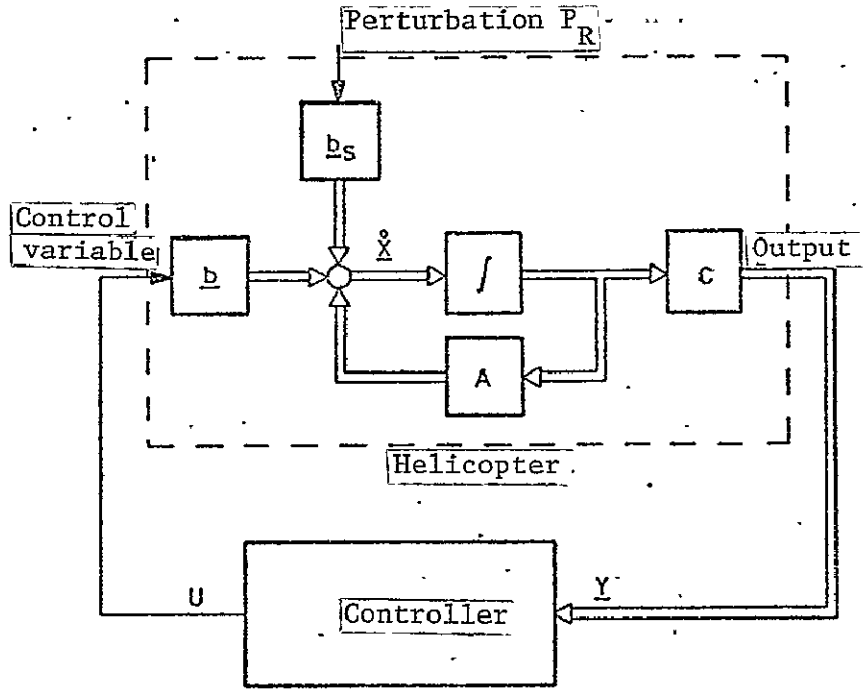

Figure 2. Block diagram of the overall systems controller.

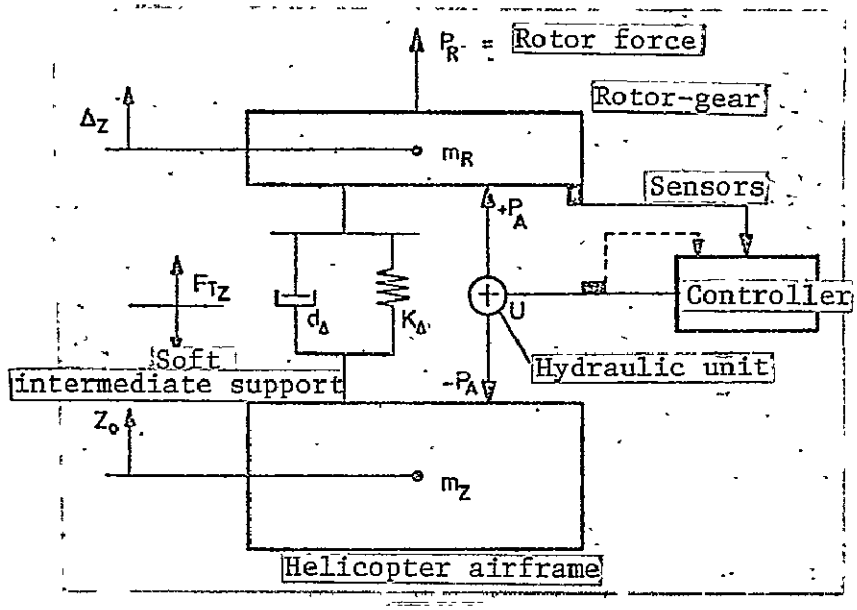

Figure 3. Helicopter model 2 for a completely active oscillation isolation system.

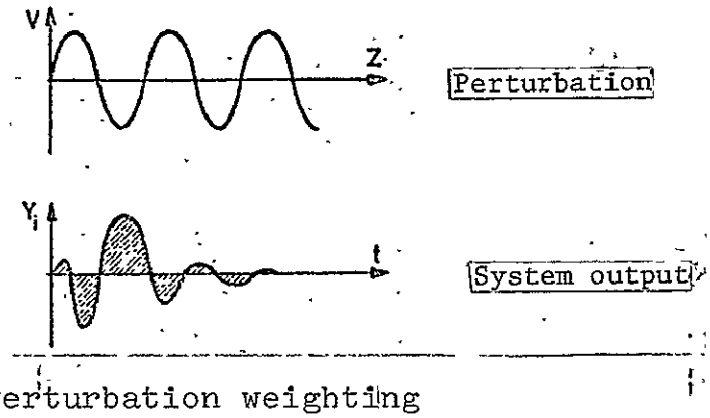

Figure 4a. Perturbation weighting

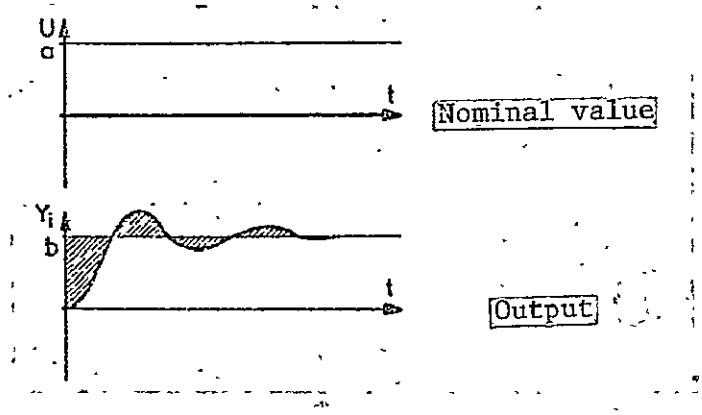

Figure 4b. Weighting of the control behavior.

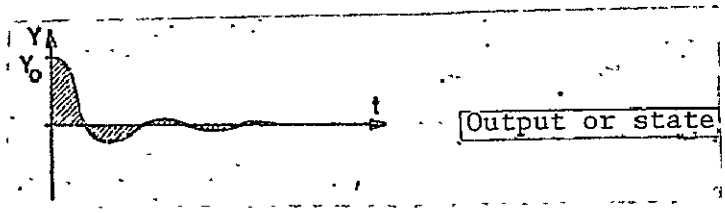

Figure 4c. Weighting of the transient behavior.

The square of the shaded area is the contribution to each quality criterion.

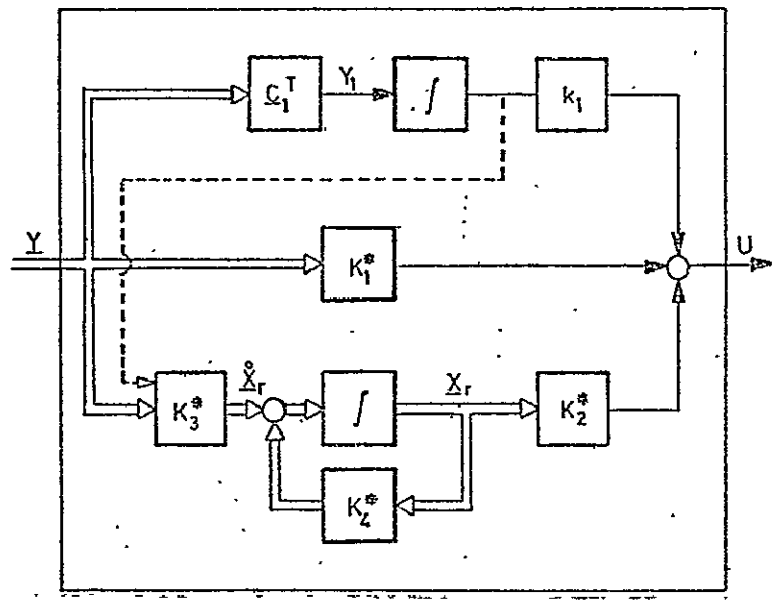

Figure 5. Controller I.

/22

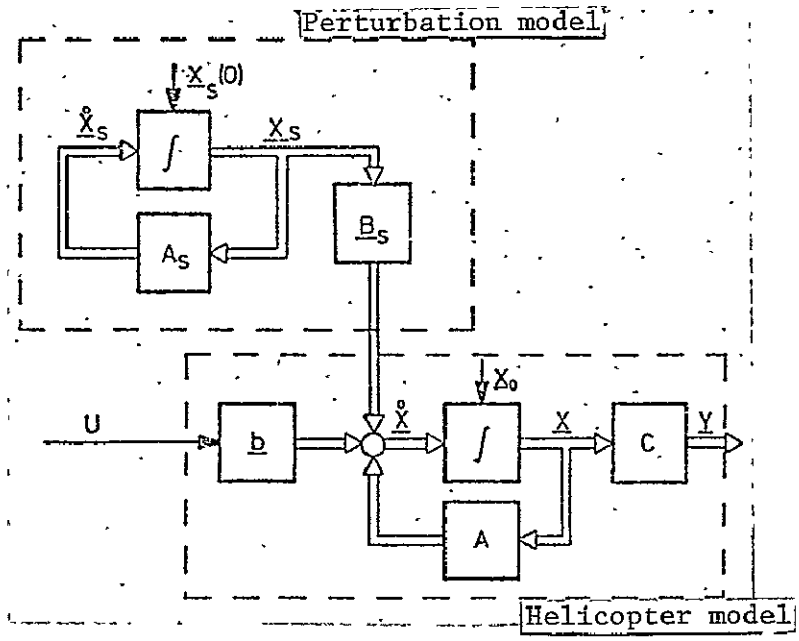

Figure 6a. Model of the helicopter with perturbation model.

/23

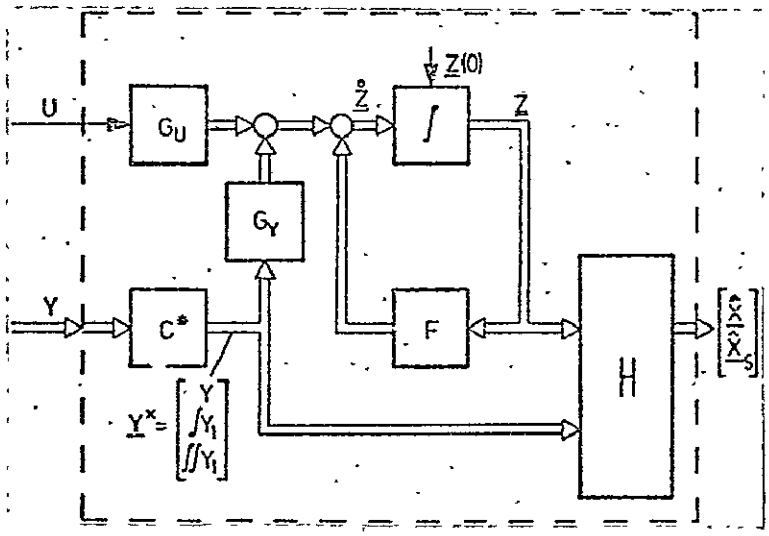

Figure 6b. Observer

ORIGINAL PAGE IS
OF POOR QUALITY

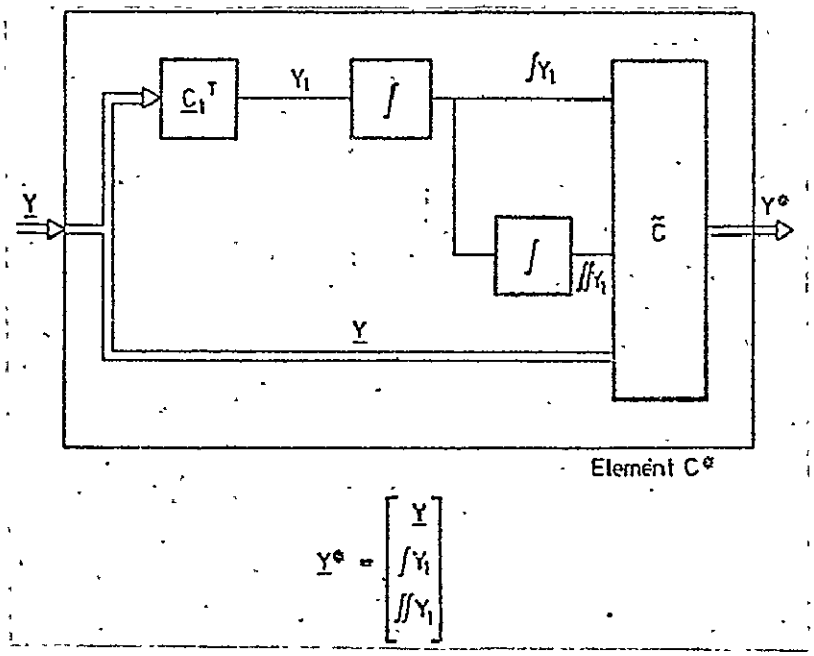

/24

Figure 6c. Structure of element C*.

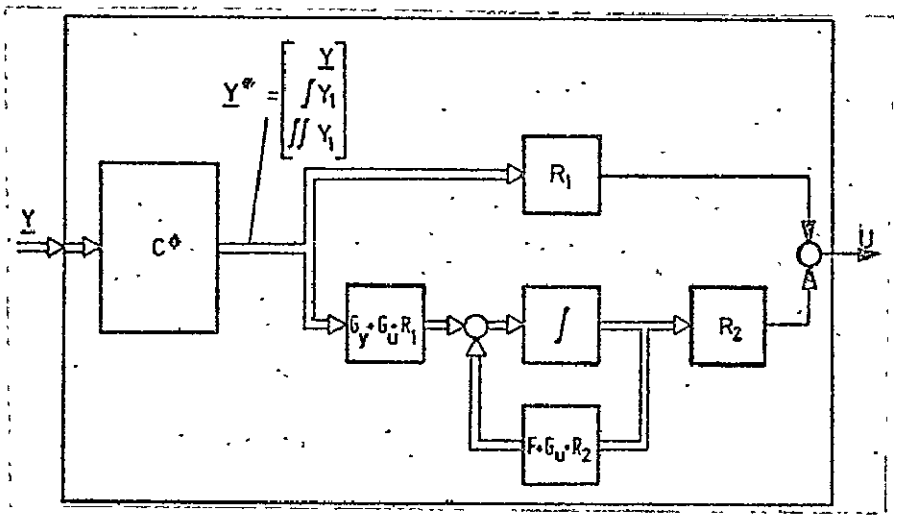

/25

Figure 7. Controller II.

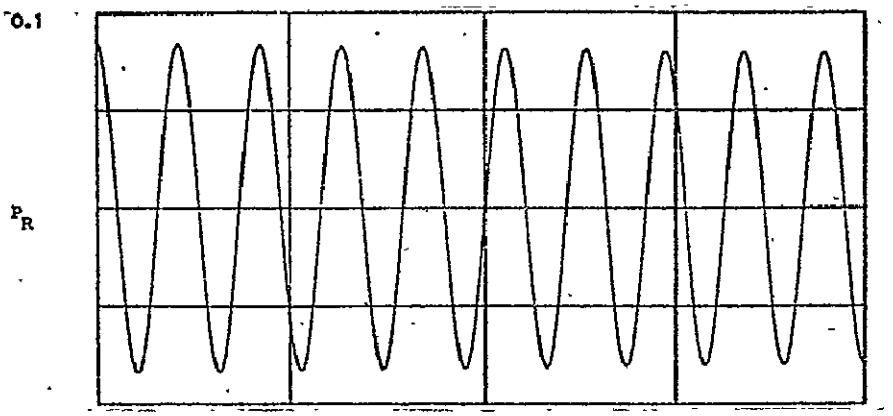

/26

Figure 8. Perturbation sequence.

Step: Perturbation compensation $\Delta T = 0.00338$ s $\Delta\psi = 0.075$ Rad
$T_{Ges} = 0.676$ s $\psi_{Ges} = 15$ Rad

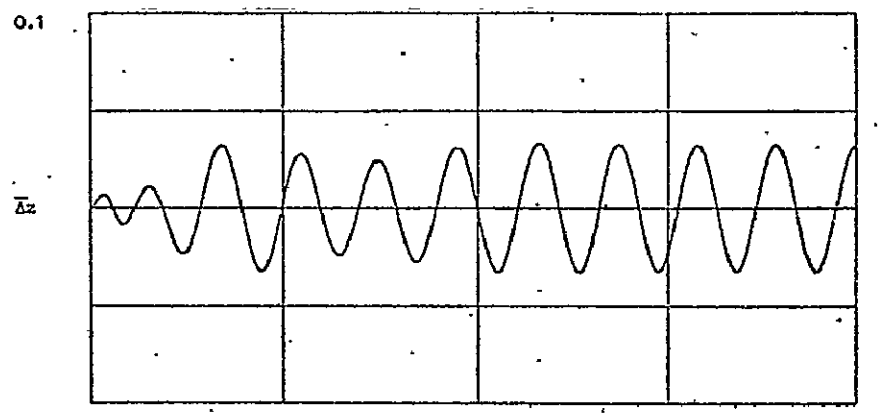

Figure 9. Variation of relative deflection

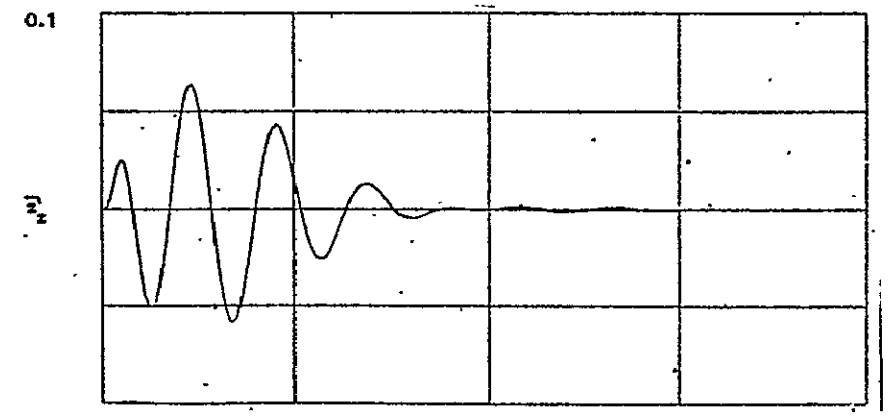

Figure 10. Variation of airframe velocity

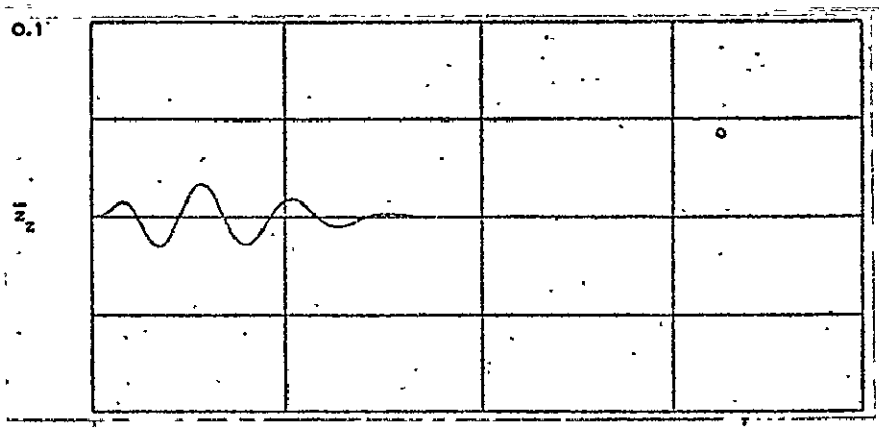

Figure 11. Variation of airframe deflection. /27

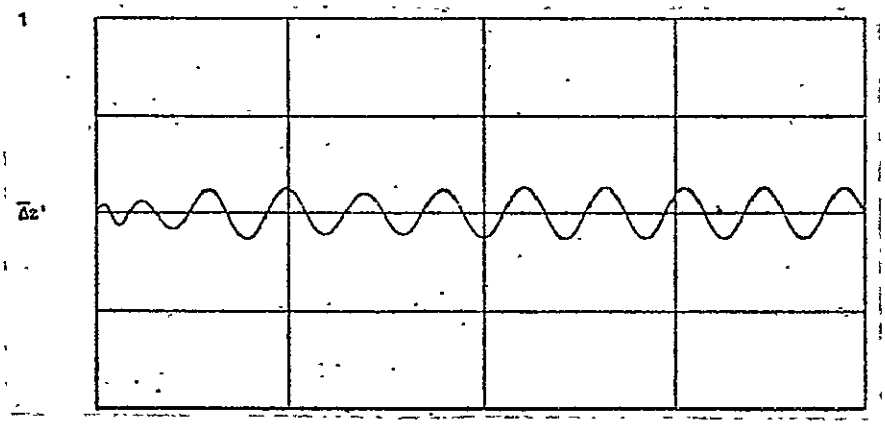

Figure 12. Velocity of relative deflection.

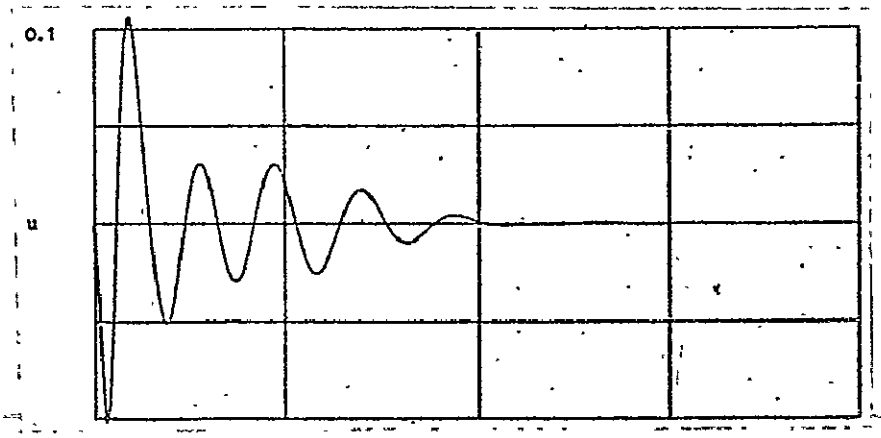

Figure 13. Control variable.

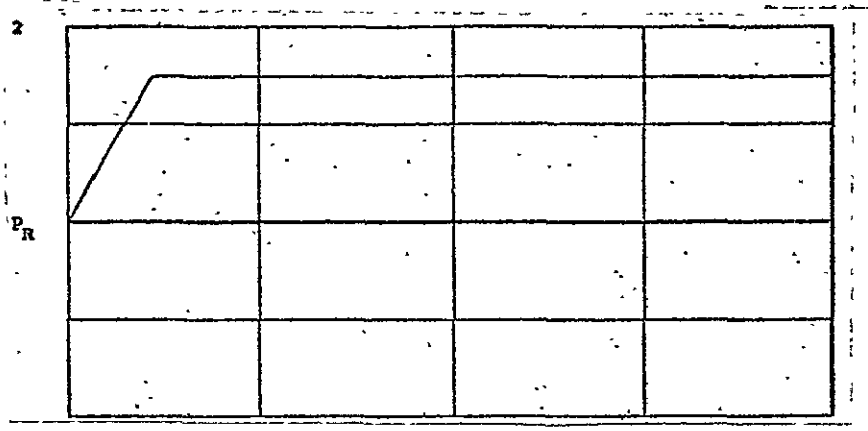

Figure 14. 2.5 g maneuver perturbation

Step: Maneuver case $\Delta T = \frac{9}{200} \triangleq \Delta\psi = 1.\text{Rad}$
$T_{Ges} = 9\ s \triangleq \psi_{Ges} = 200\ \text{Rad}$

/28

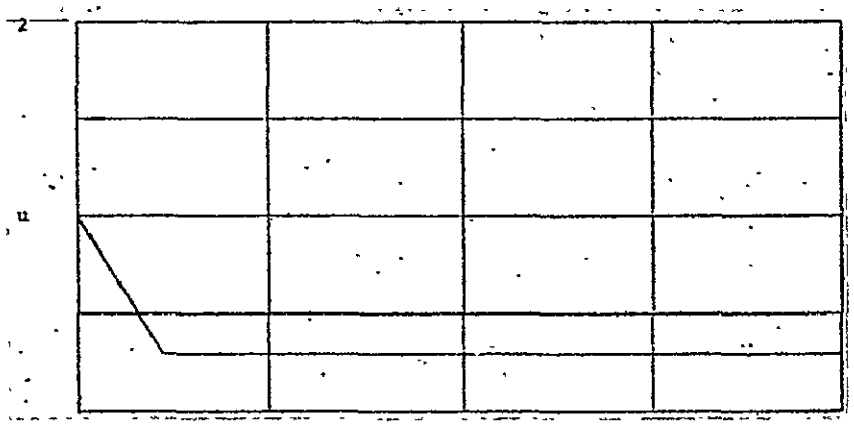

Figure 15. Control variable

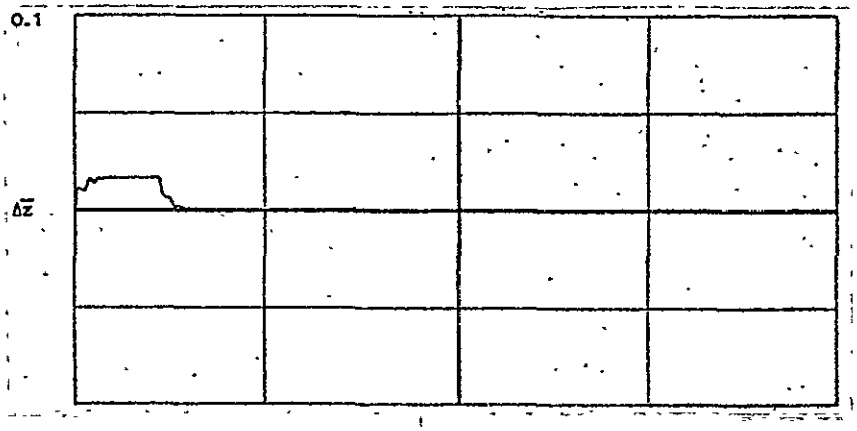

Figure 16. Variation of relative deflection.

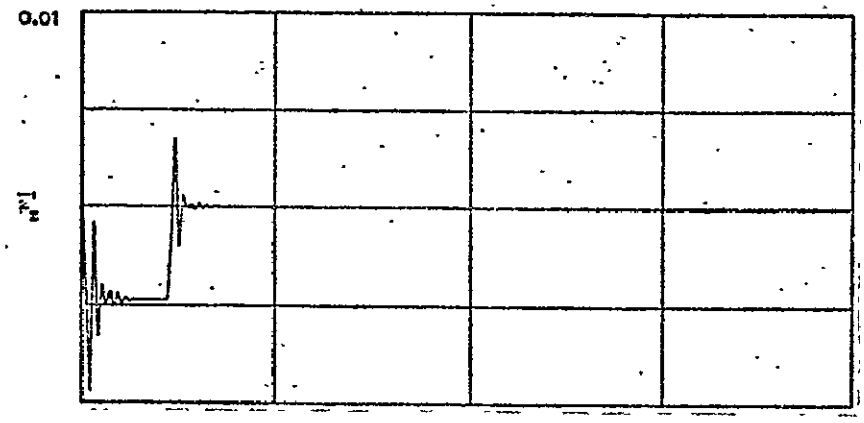

/29

Figure 17. Airframe velocity.

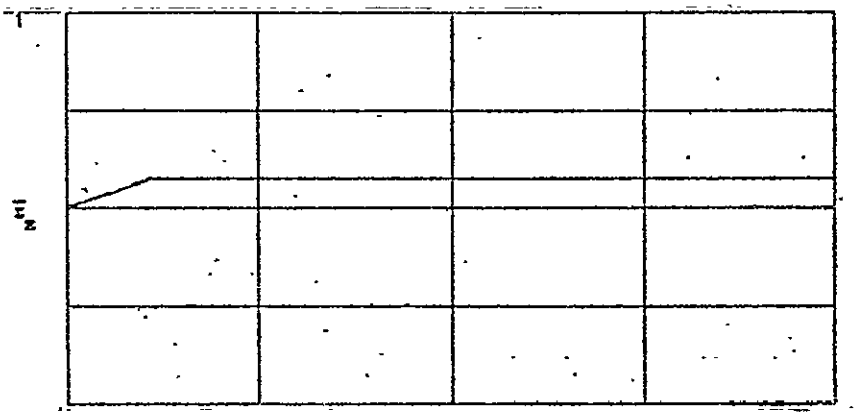

Figure 18. Variation of airframe deflection.

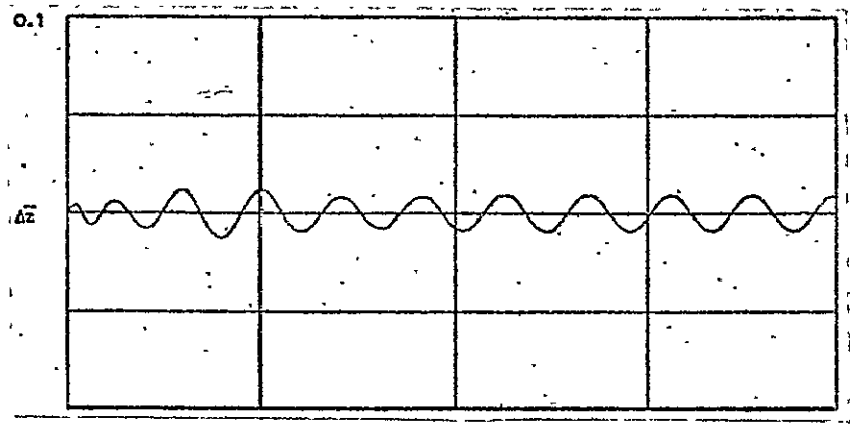

Figure 19. Relative deflection.

/ 30

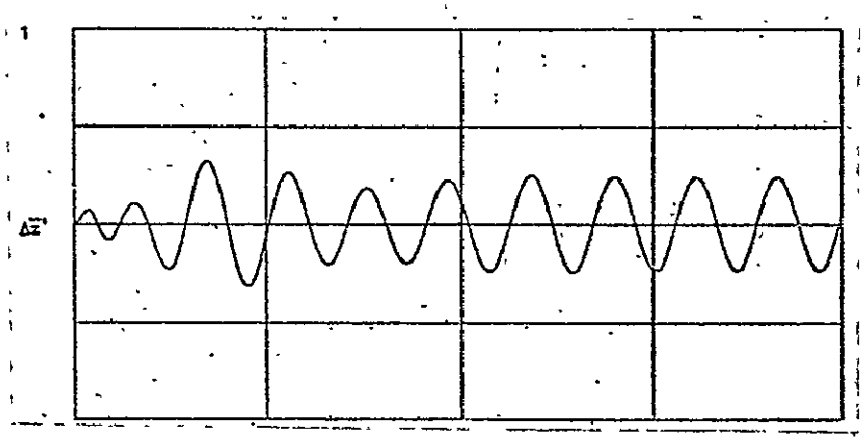

Figure 20. Velocity of relative deflection.

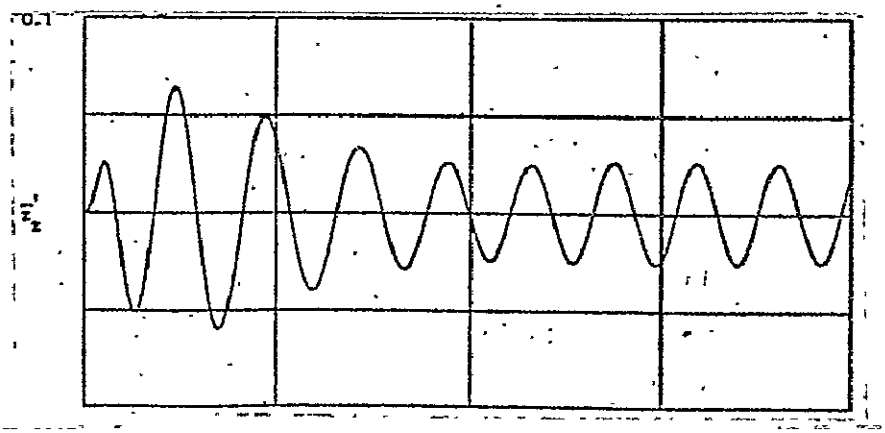

Figure 21. Airframe velocity

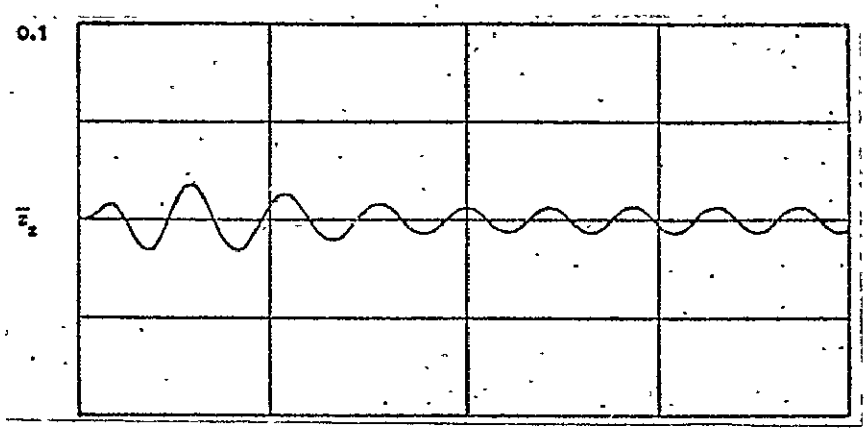

/ 31

Figure 22. Airframe deflection

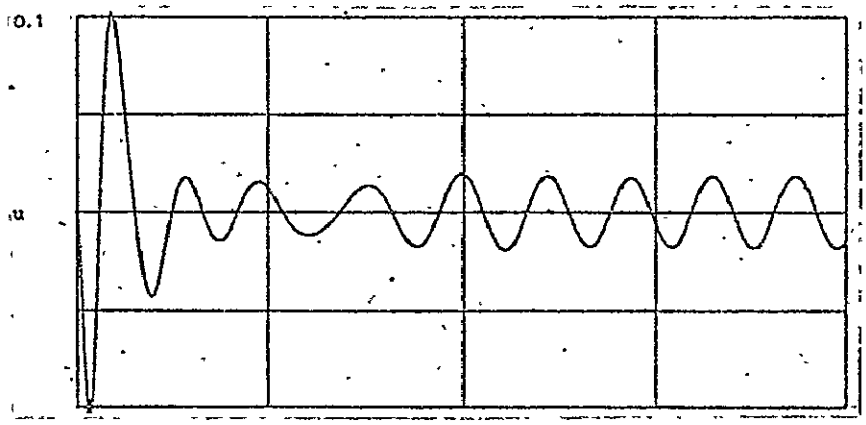

Figure 23. Control variable.

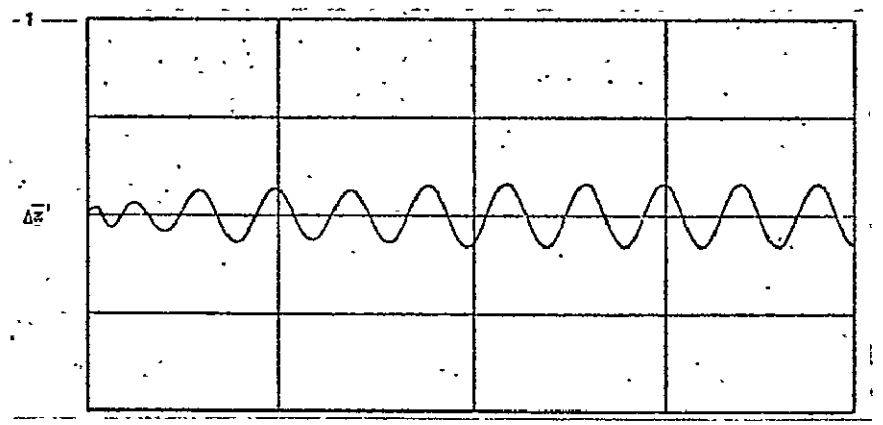

Figure 24. Relative deflection velocity.

/ 32

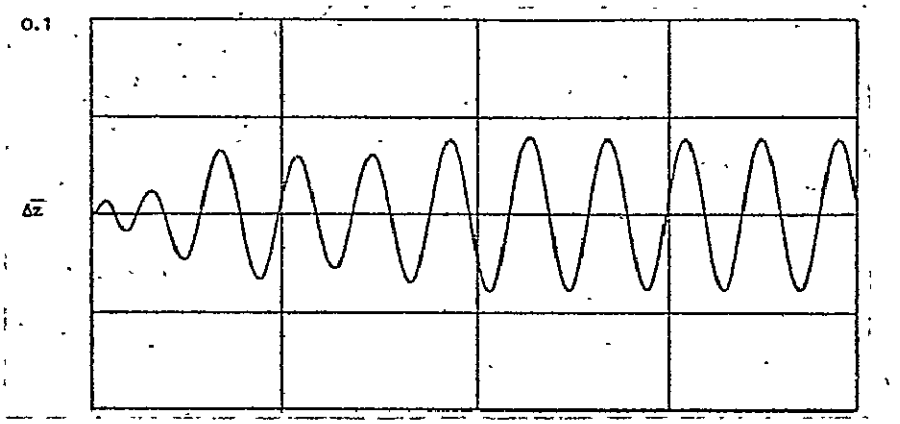

Figure 25. Relative deflection.

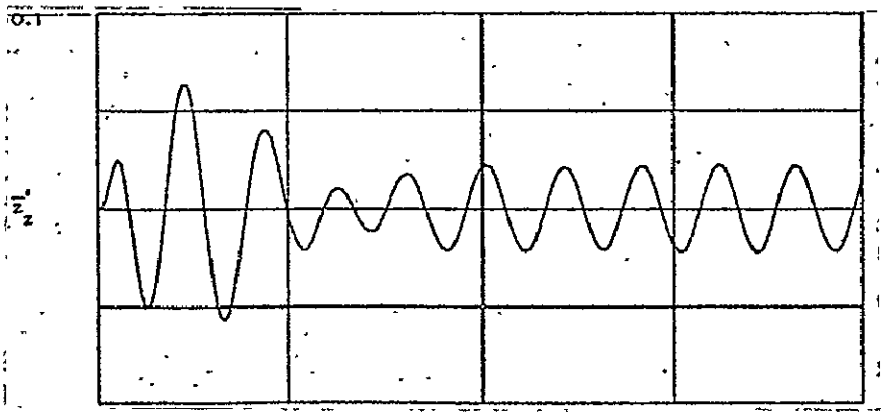

Figure 26. Airframe velocity

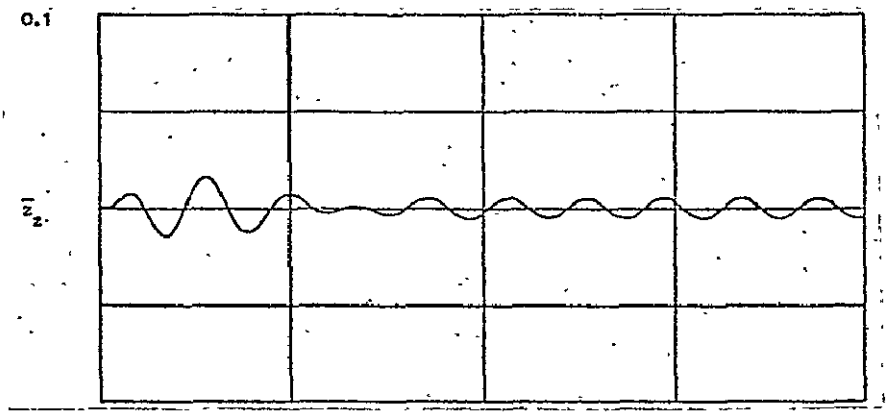

/ 33

Figure 27. Airframe deflection.

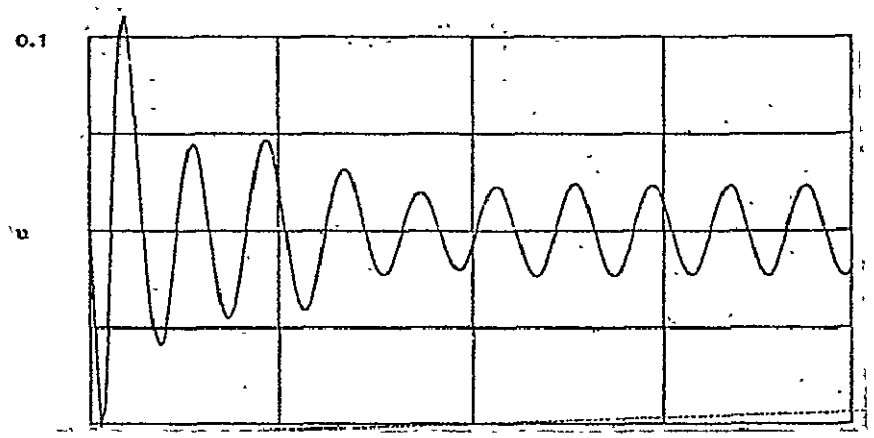

Figure 28. Control variable.

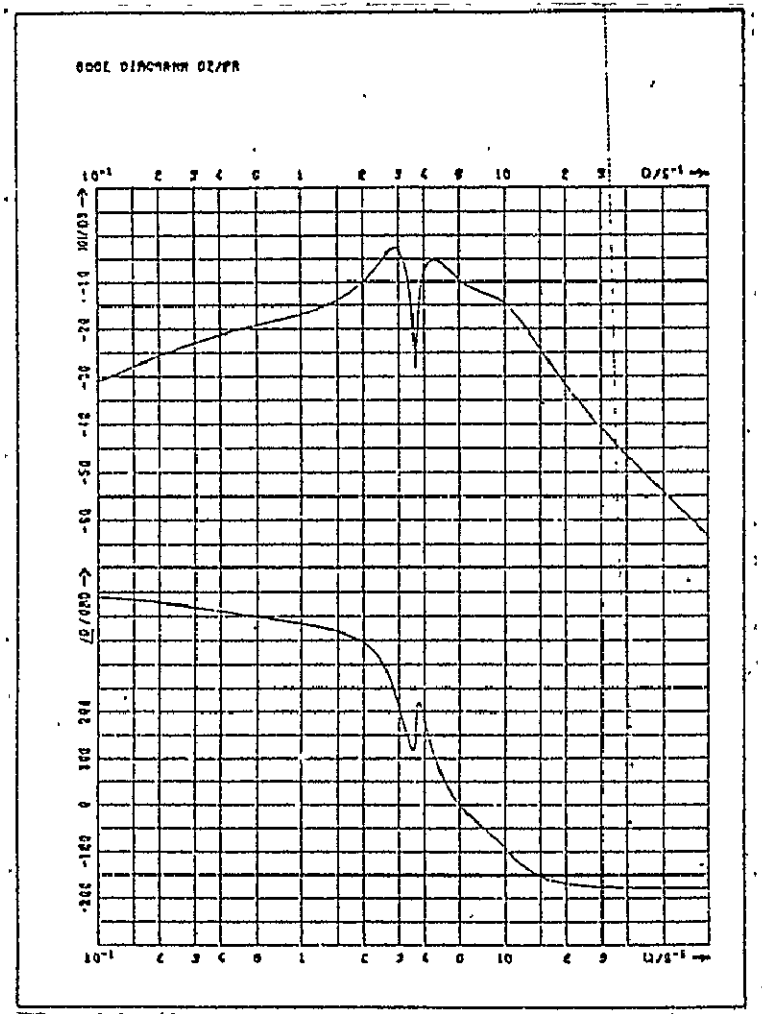

Figure 29. Bode diagram of perturbation transfer function of relative deflection

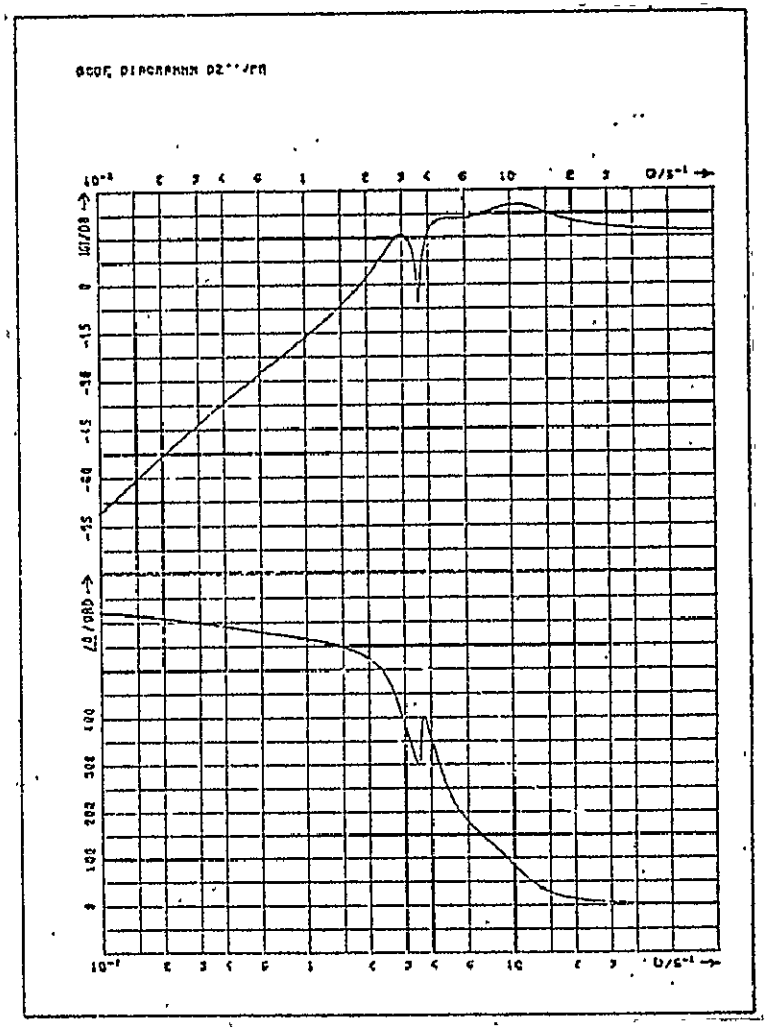

Figure 30. Bode diagram of perturbation transfer function of relative acceleration.

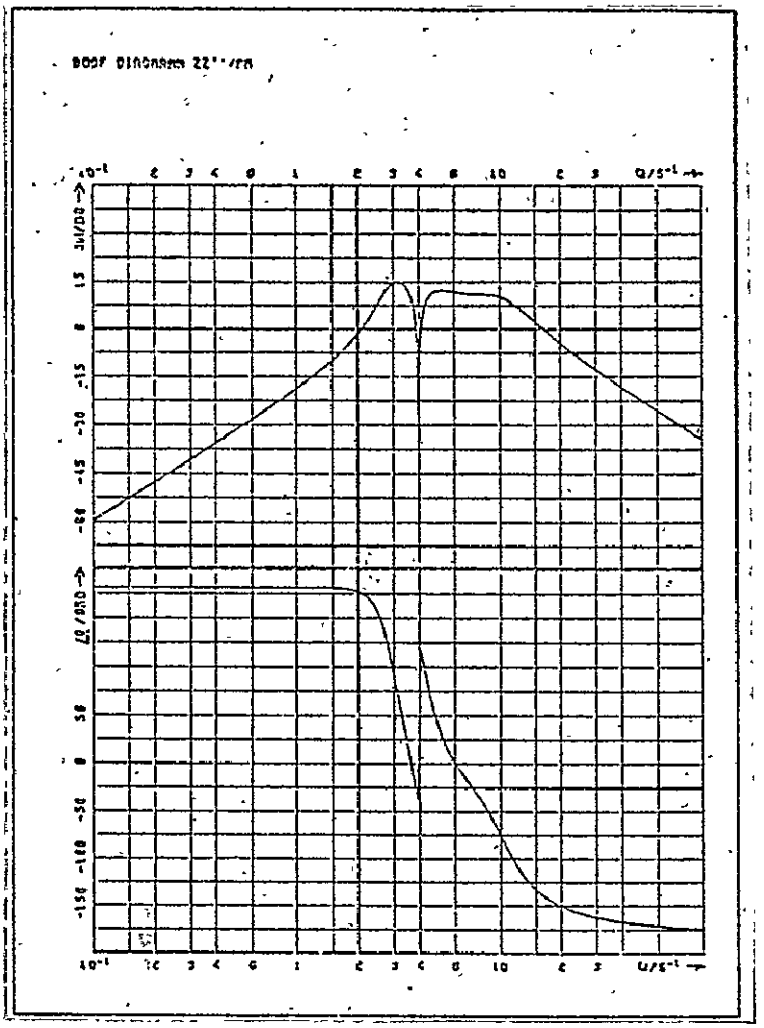

Figure 31. Bode diagram of perturbation transfer function of airframe acceleration.

/35

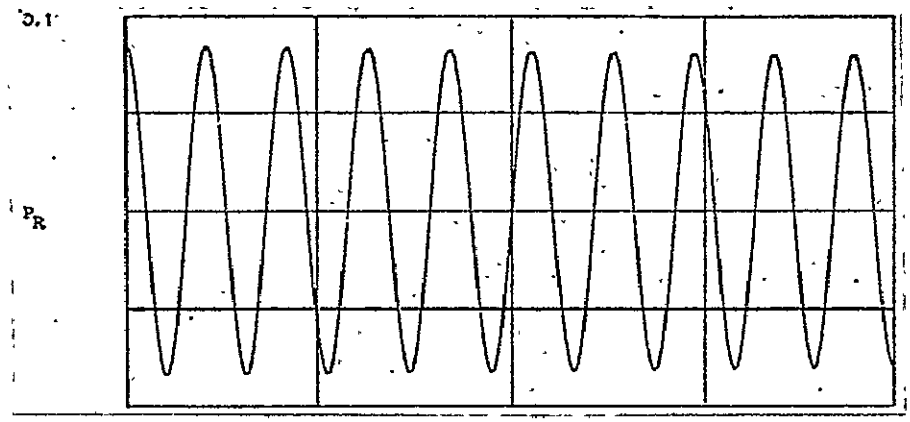

Figure 32. Perturbation.

/ 36

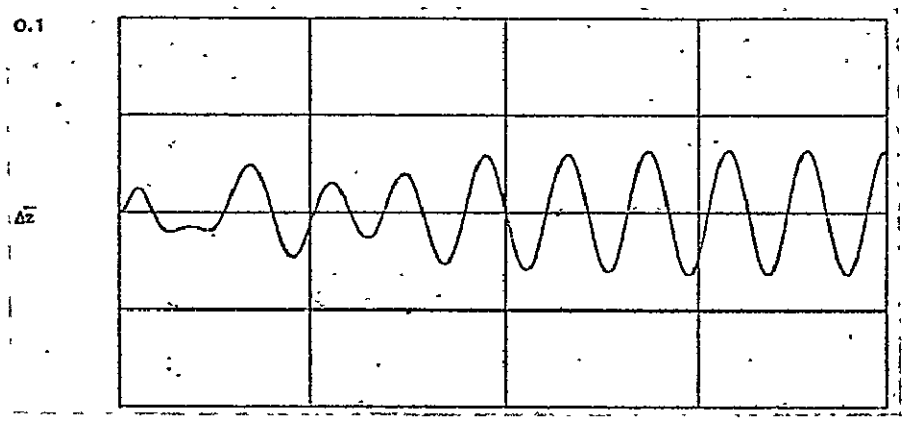

Figure 33. Relative deflection.

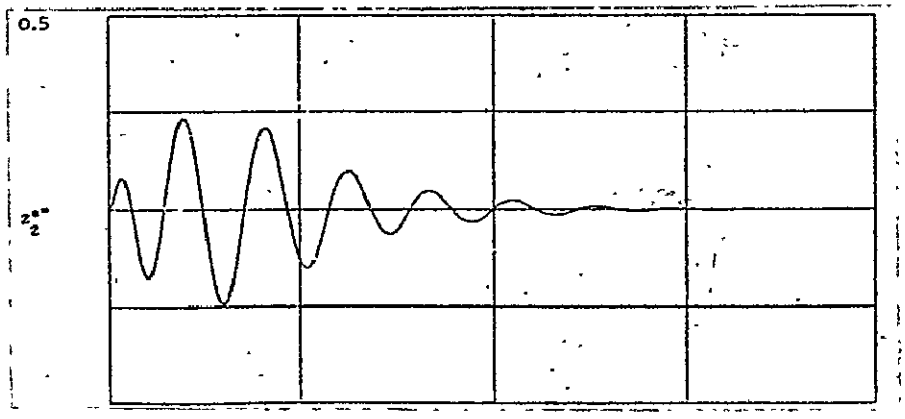

Figure 34. Delayed airframe acceleration.

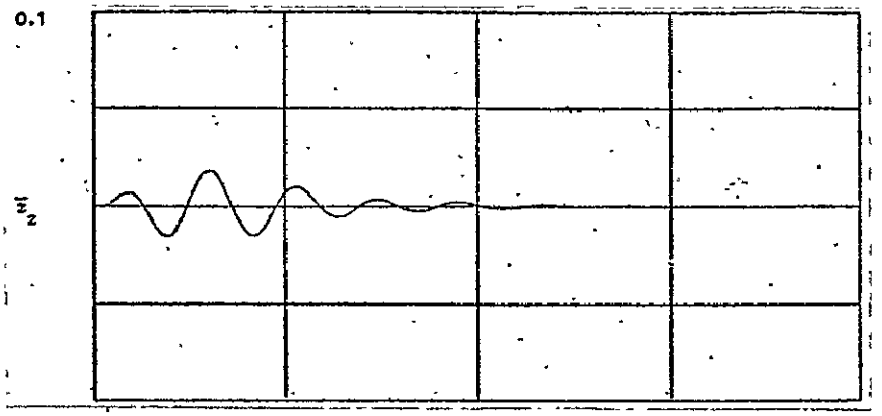

Figure 35. Airframe deflection.

/37

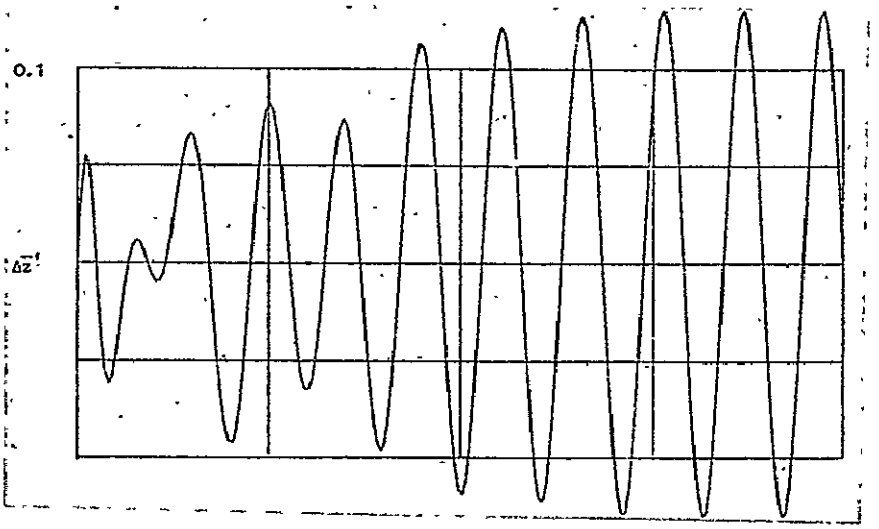

Figure 36. Velocity of relative deflection.

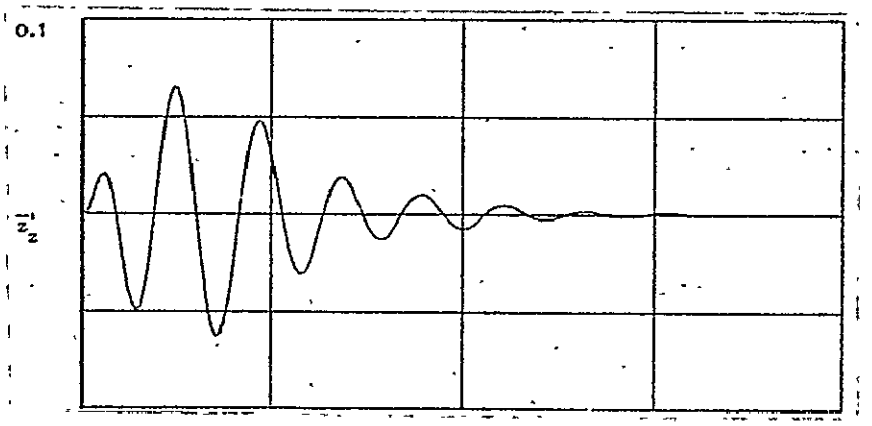

Figure 37. Airframe velocity.

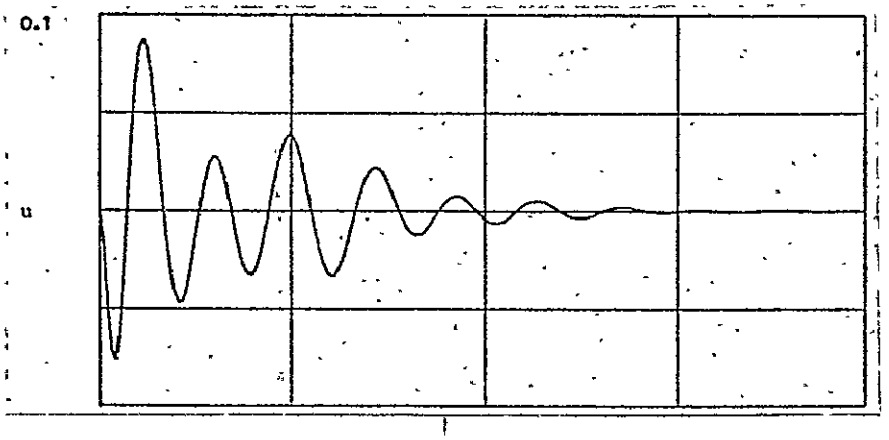

/38

Figure 38. Control variable.

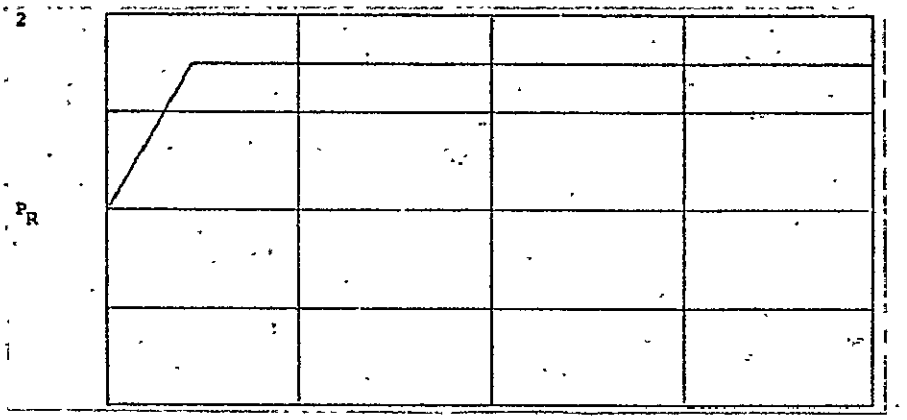

Figure 39. 2.5 g maneuver perturbation.

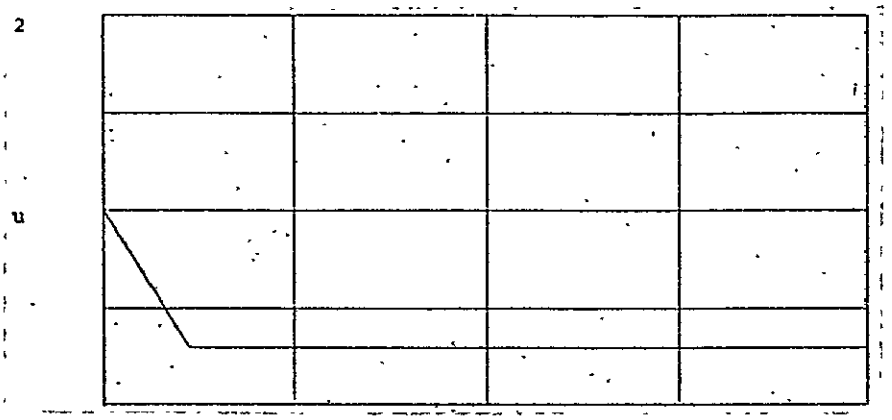

Figure 40. Control variable.

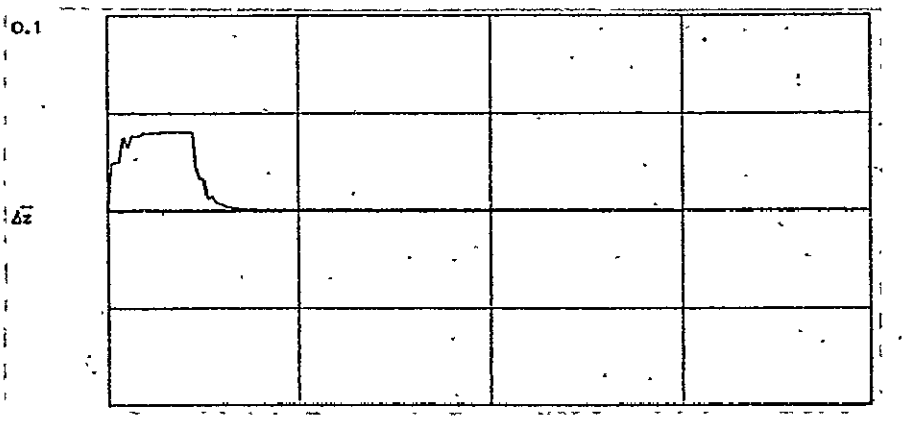

Figure 41. Relative deflection.

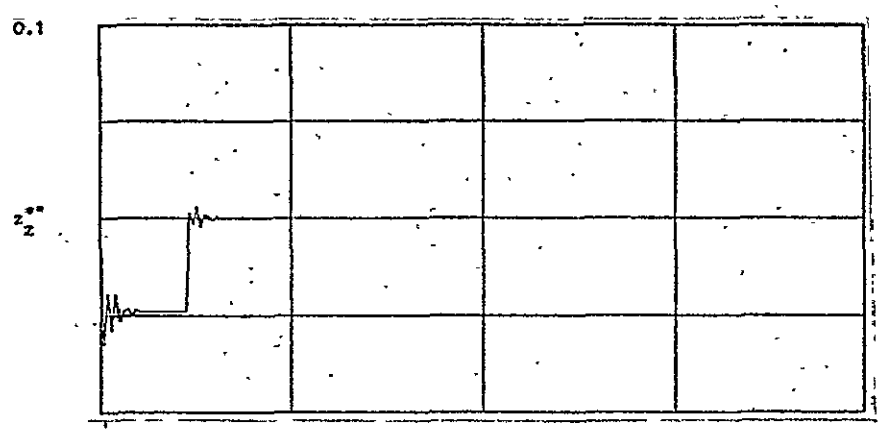

Figure 42. Delayed airframe acceleration.

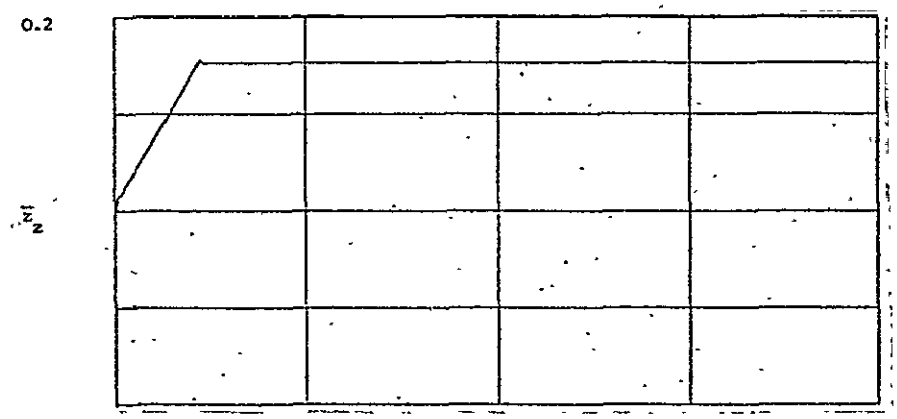

Figure 43. Airframe deflection.

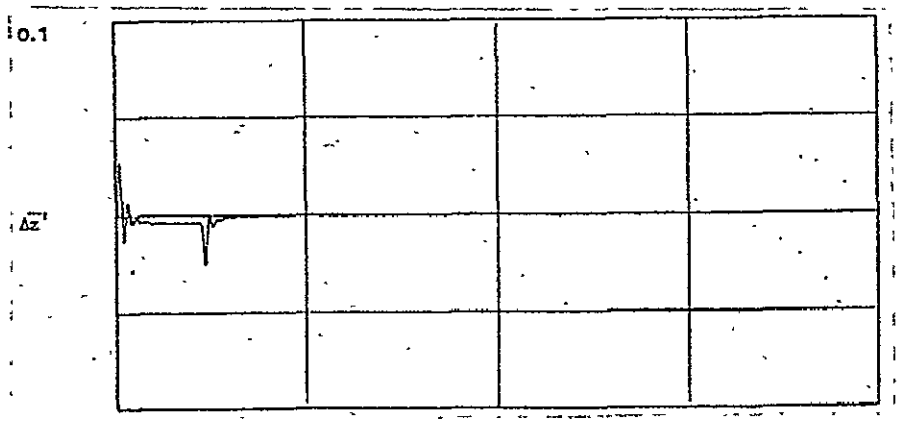

Figure 44. Relative deflection velocity.

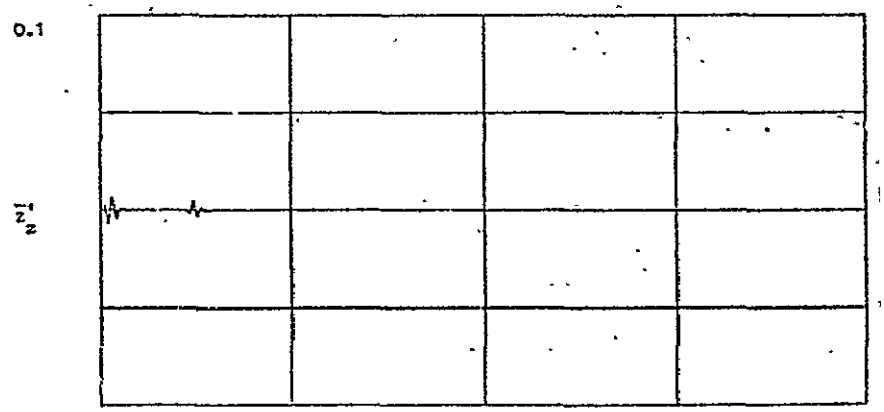

Figure 45. Airframe velocity.

Figure 46. Bode diagram of perturbation transfer function of relative motion.

Figure 47. Bode diagram of perturbation transfer function of relative acceleration.

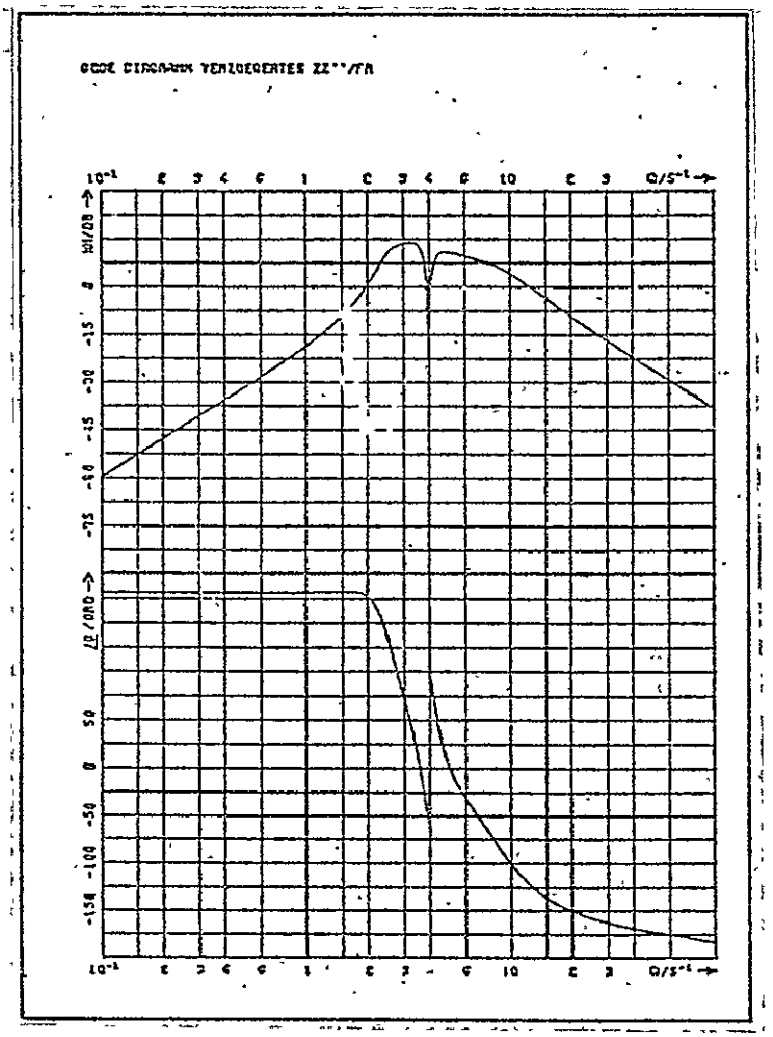

Figure 48. Bode diagram of perturbation transfer function of delayed airframe acceleration.

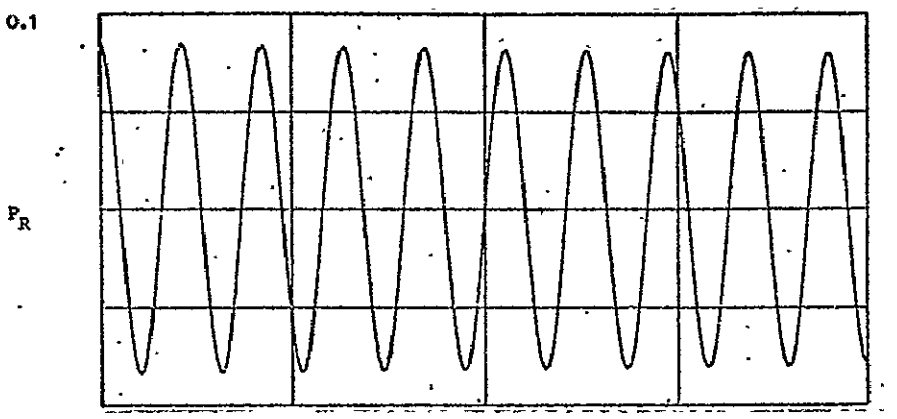

Figure 49. Perturbation.

/44

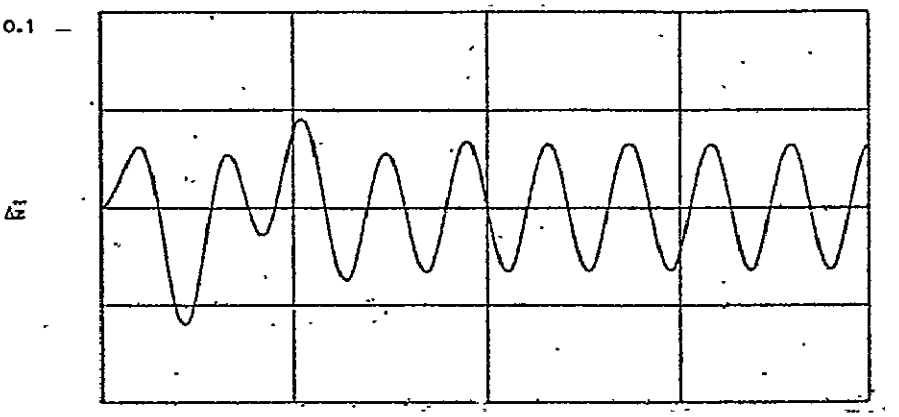

Figure 50. Relative deflection

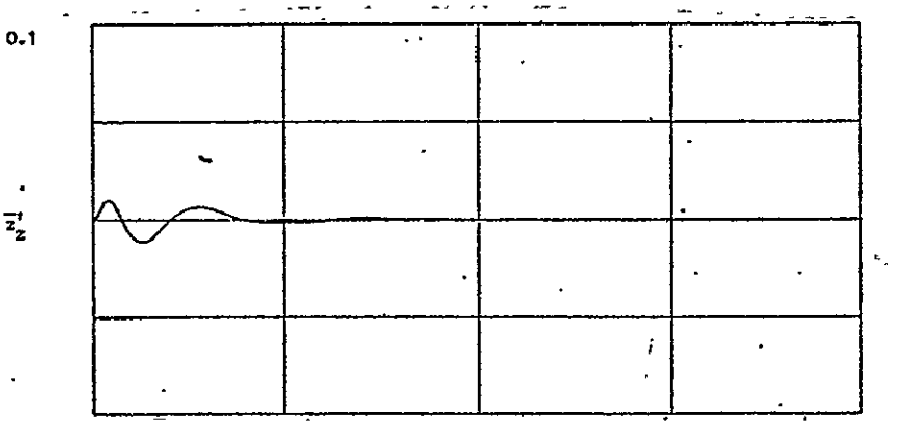

Figure 51. Airframe velocity.

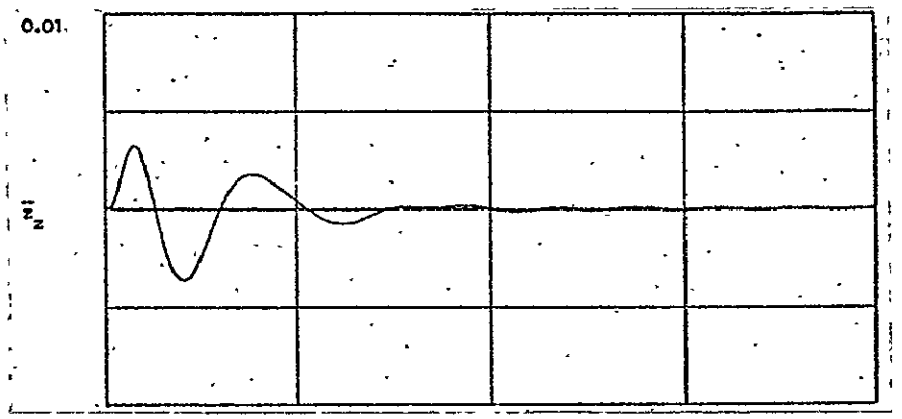

Figure 52. Air frame deflection.

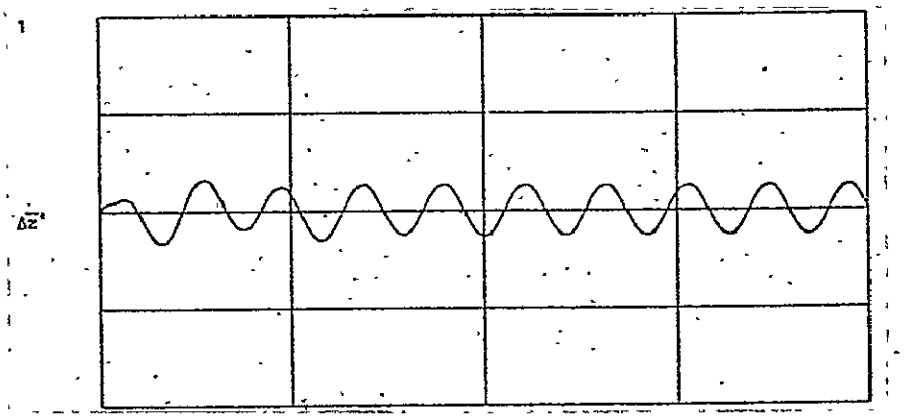

Figure 53. Relative deflection velocity.

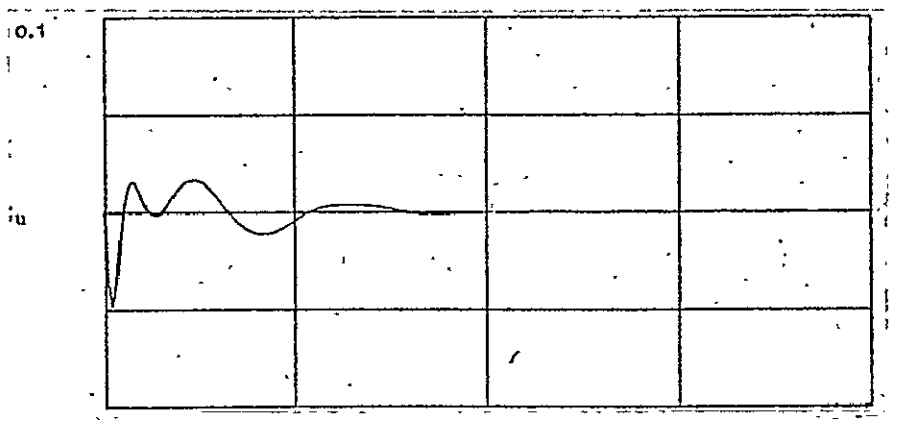

Figure 54. Control variable

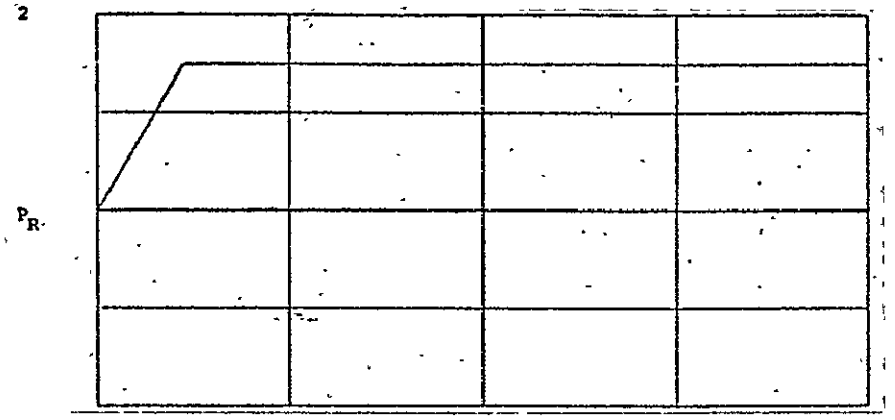

Figure 55. 2.5 g maneuver perturbation. /46

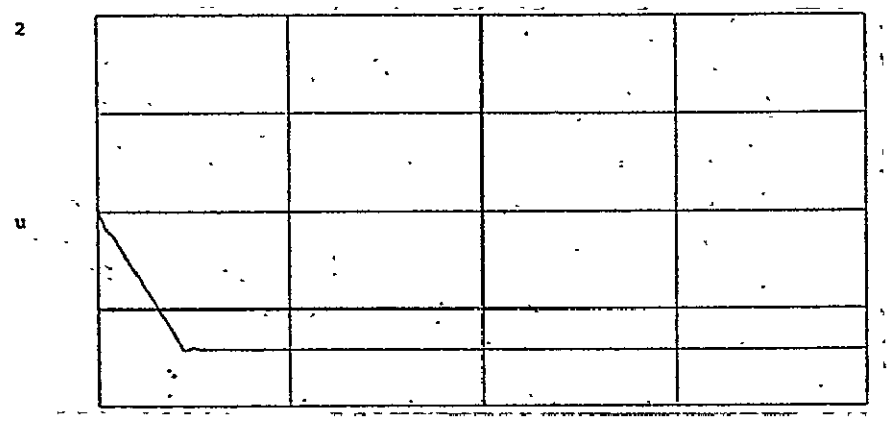

Figure 56. Control variable.

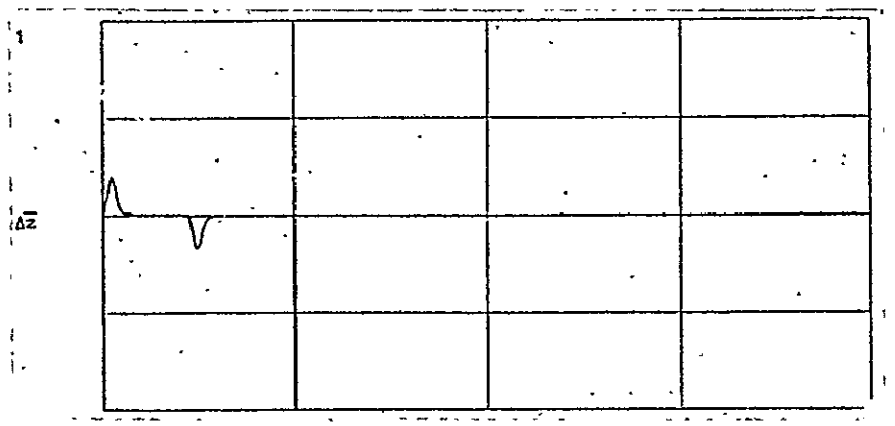

Figure 57. Relative deflection.

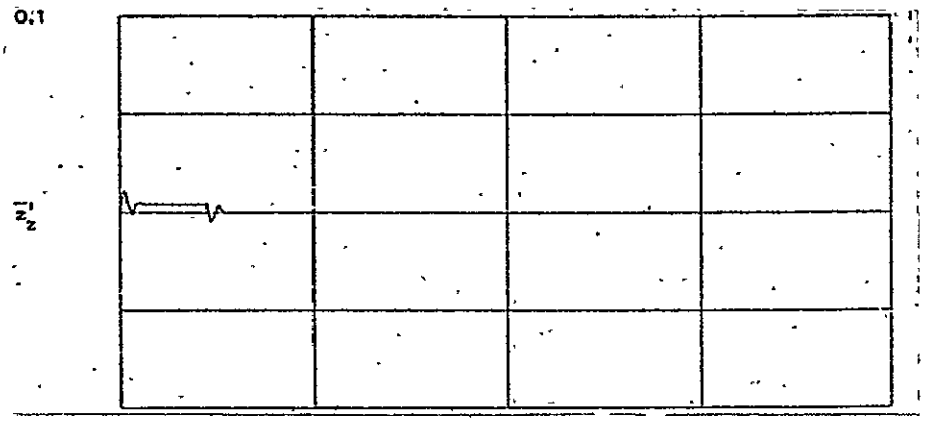

Figure 58. Airframe velocity.

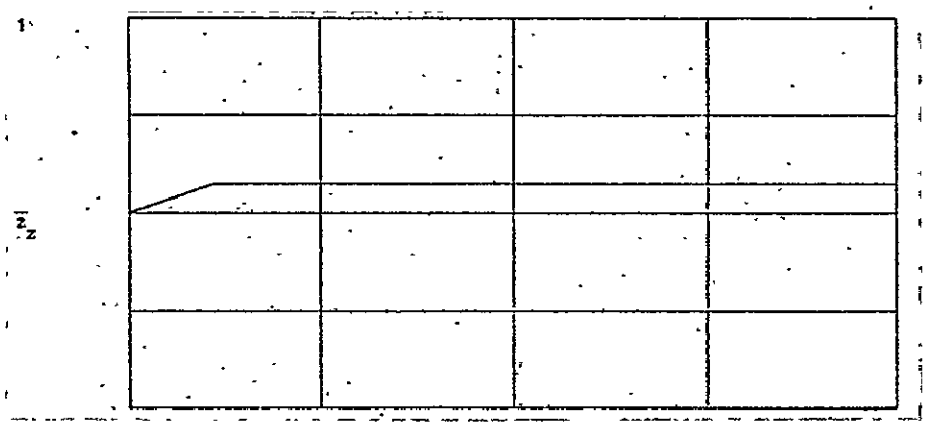

Figure 59. Airframe deflection.

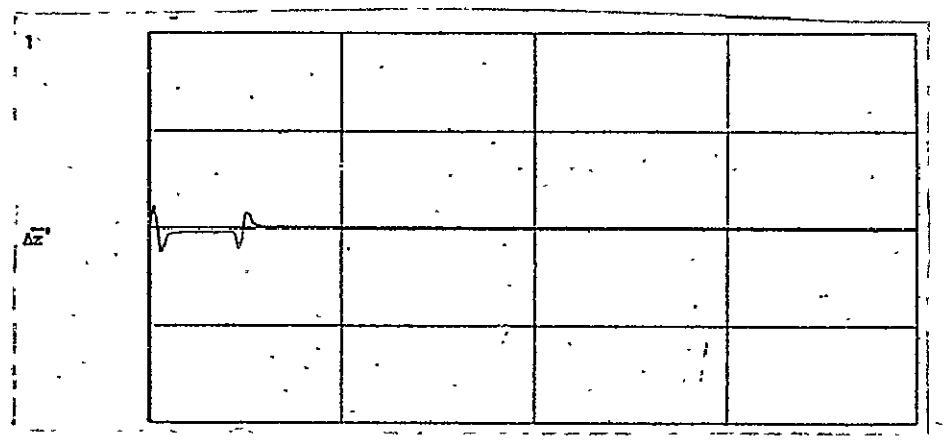

Figure 60. Relative deflection velocity.

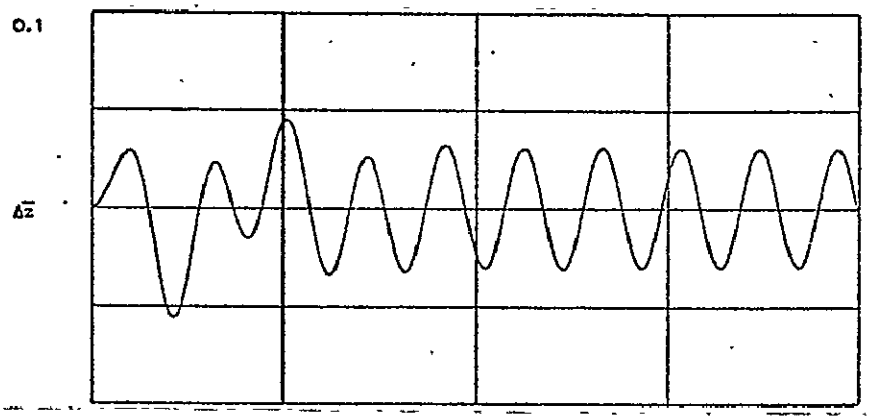

Figure 61. Relative deflection.

/48

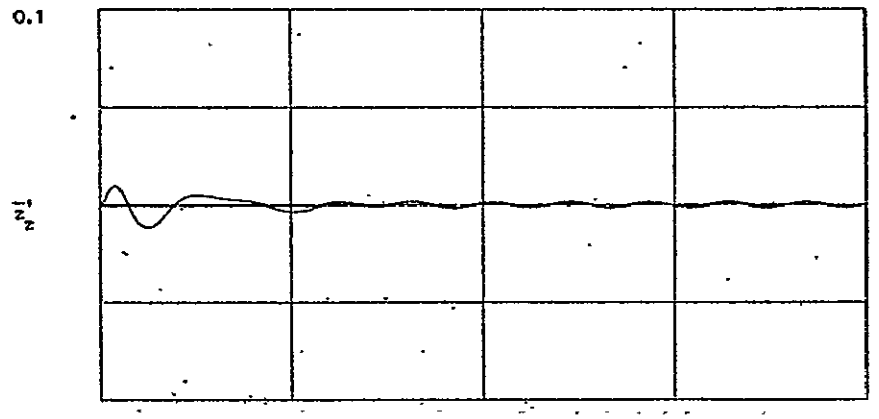

Figure 62. Airframe velocity.

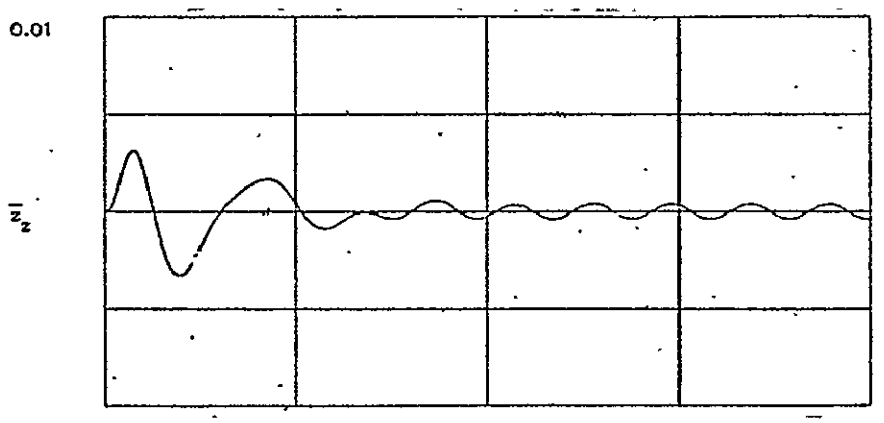

Figure 63. Airframe deflection.

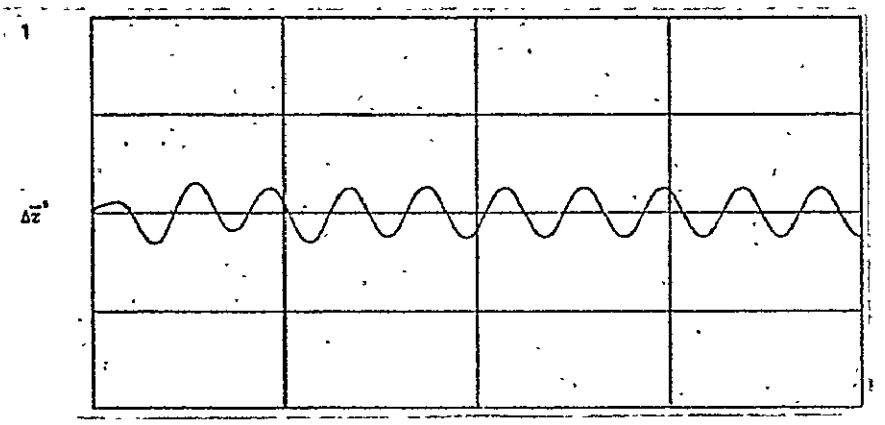

/49

Figure 64. Velocity of relative deflection.

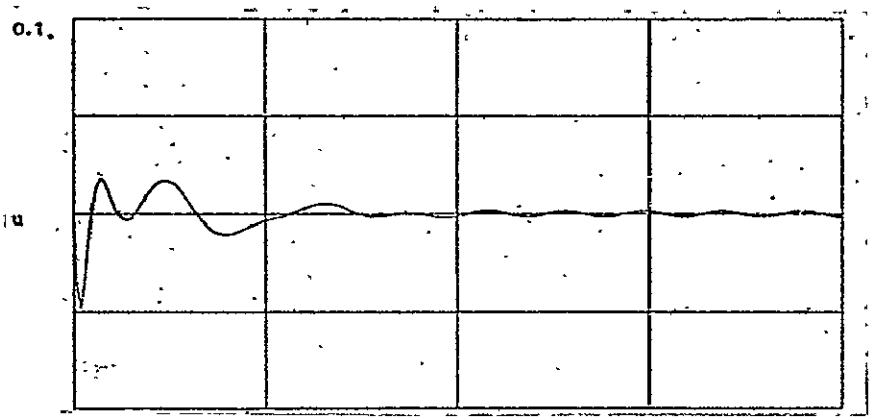

Figure 65. Control variable.

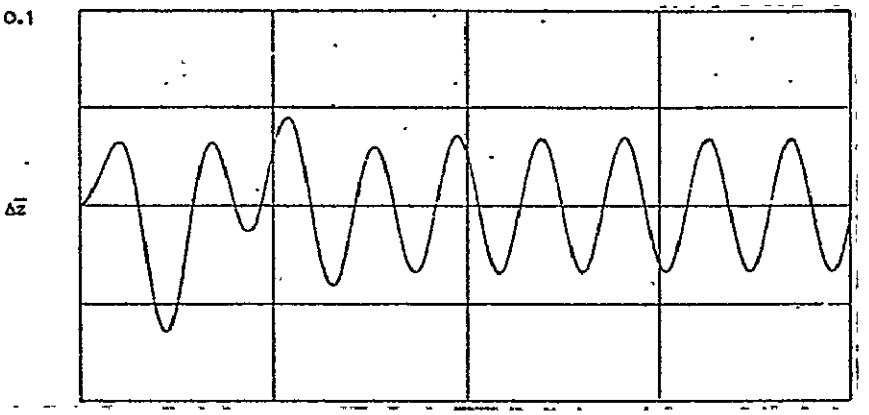

Figure 66. Relative deflection.

/50

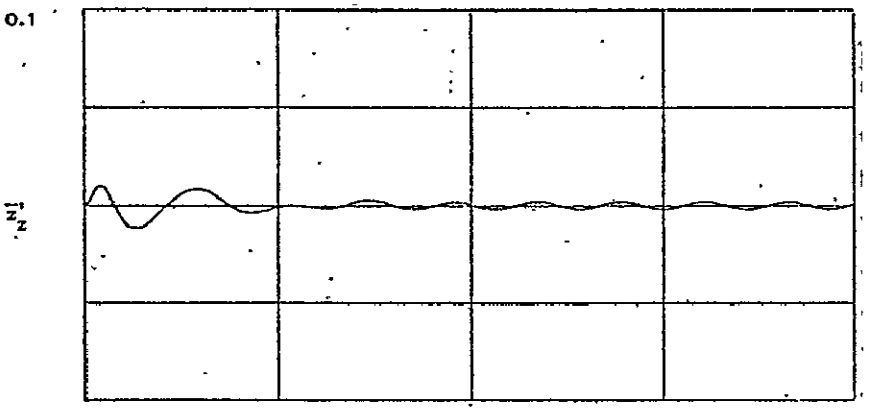

Figure 67. Airframe velocity.

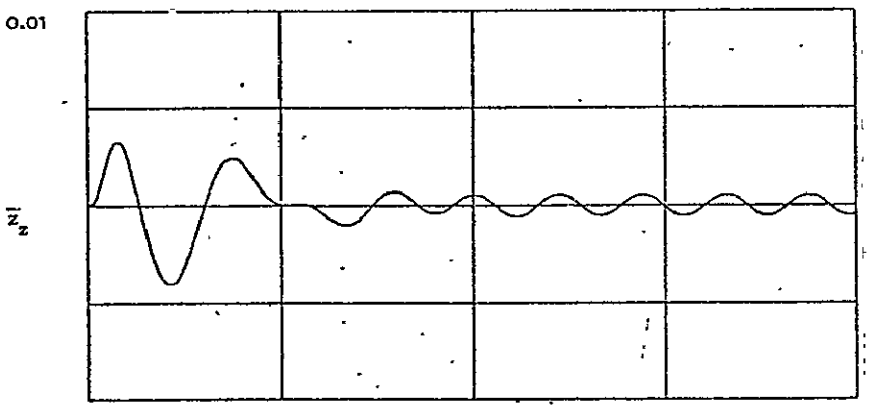

Figure 68. Airframe deflection

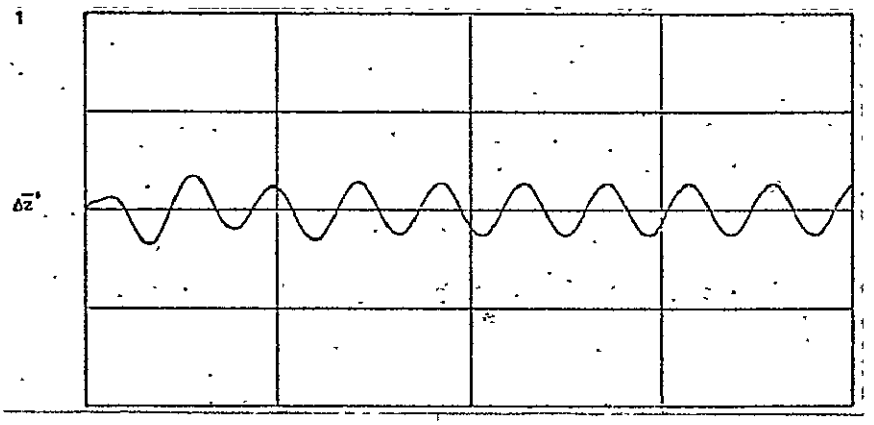

Figure 69. Velocity of relative deflection.

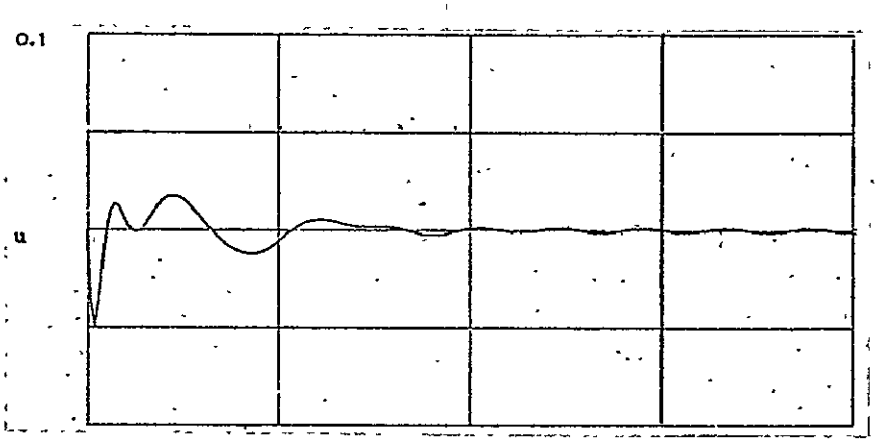

Figure 70. Control variable.

Figure 71. Bode diagram of the perturbation transfer function of relative deflection.

Figure 72. Bode diagram of the perturbation transfer function of relative acceleration.

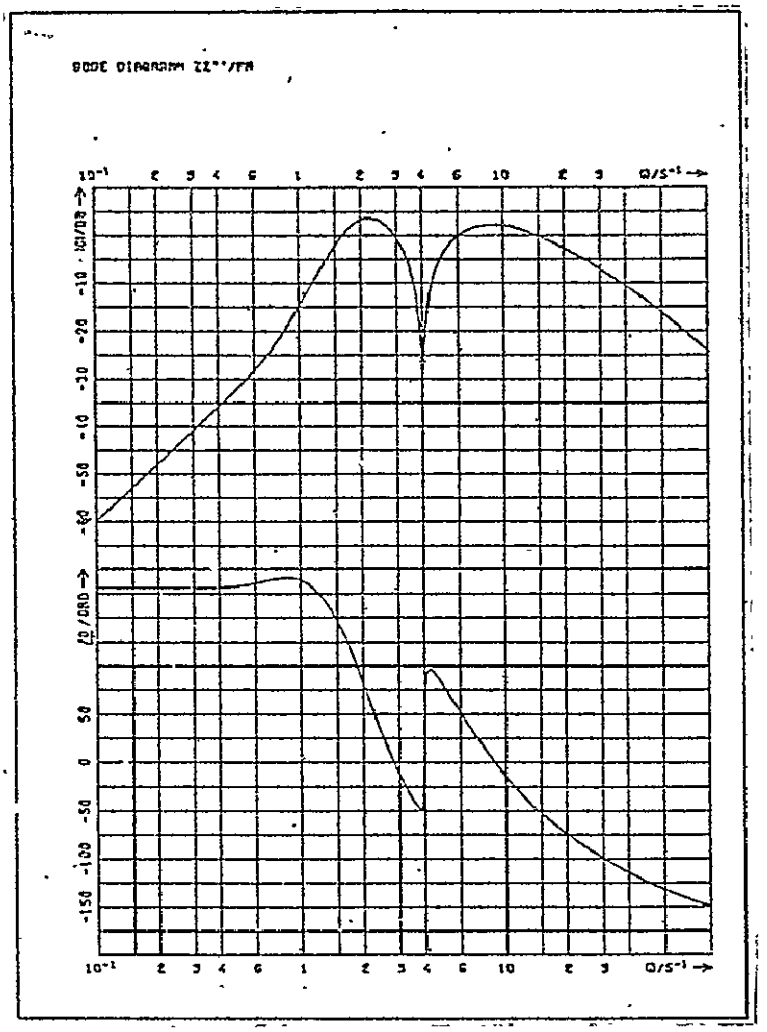

Figure 73. Bode diagram of the perturbation transfer function of airframe acceleration.

/53

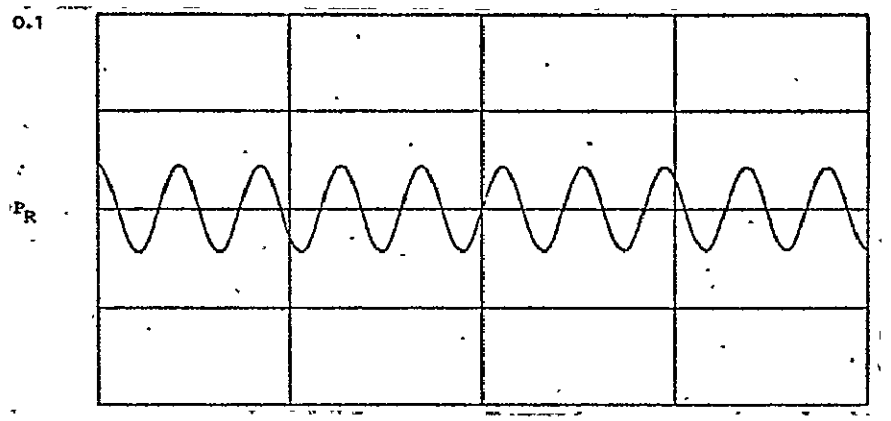

Figure 74. Perturbation sequence.

/54

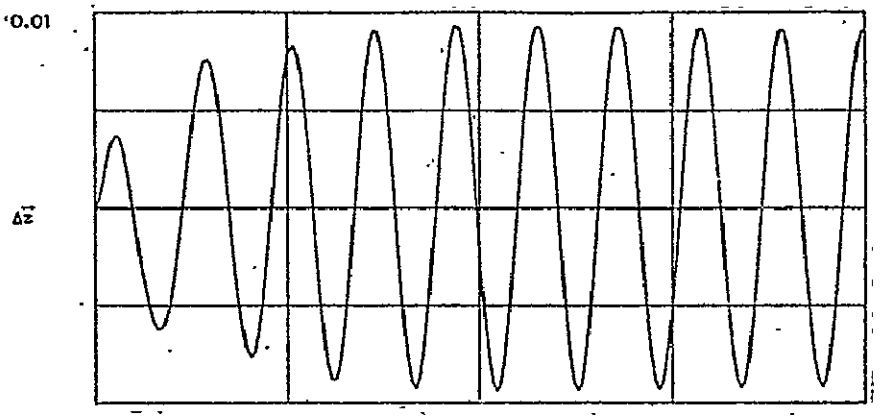

Figure 75. Relative deflection.

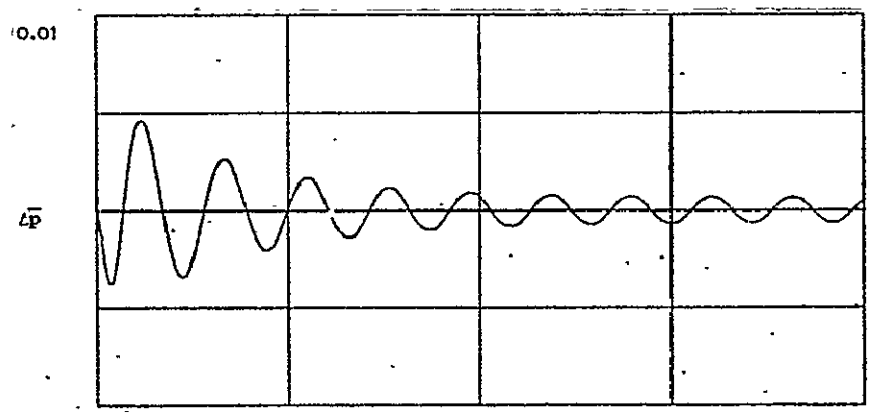

Figure 76. Differential pressure of actuator.

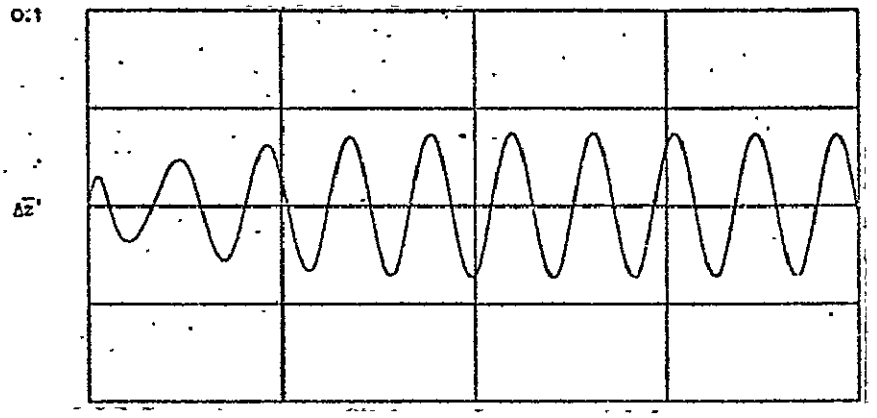

Figure 77. Relative deflection velocity.

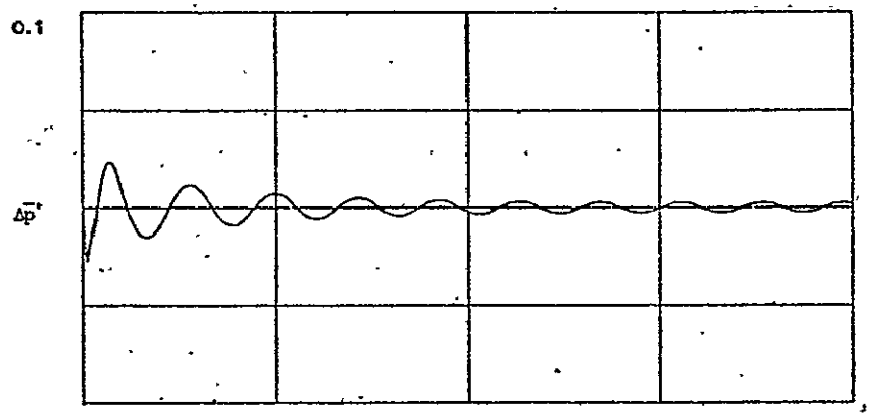

Figure 78. Derivative of differential pressure.

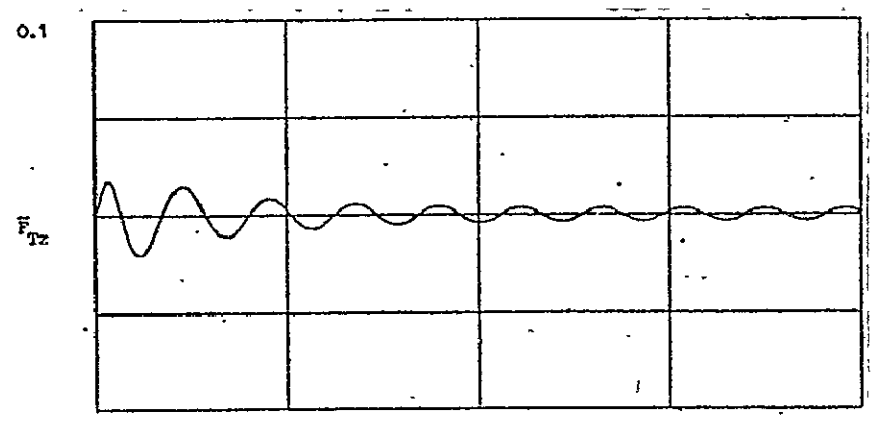

Figure 79. Isolator force.

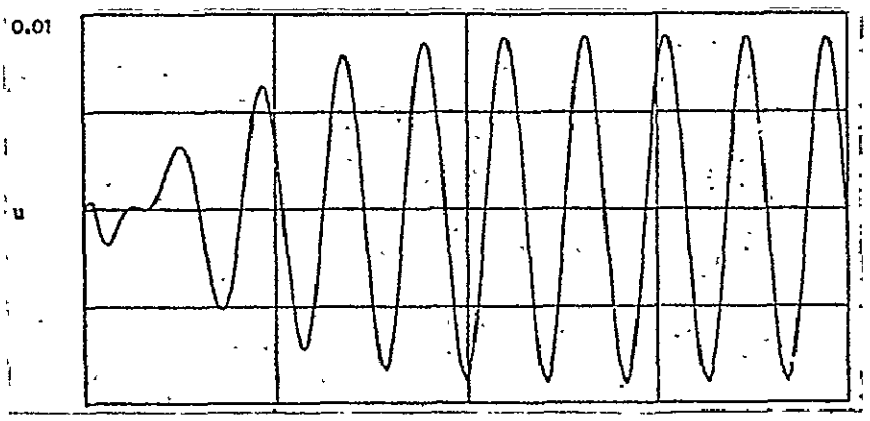

/ 56

Figure 80. Control variable.

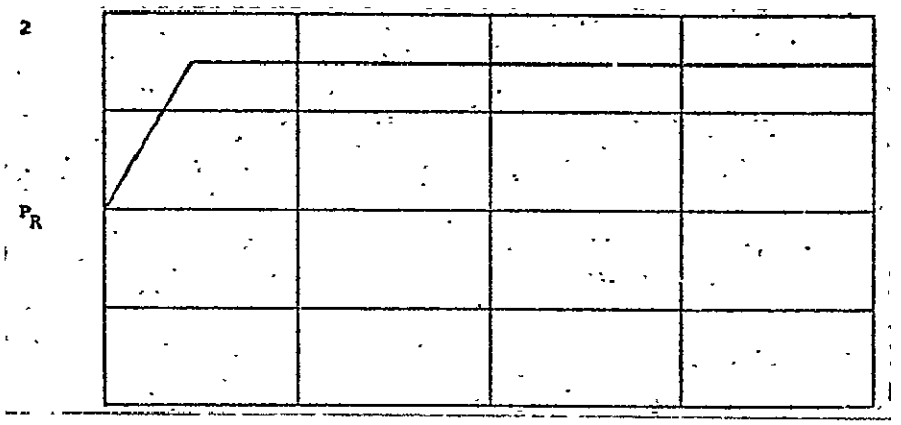

Figure 81. 2.5 g maneuver perturbation. /57

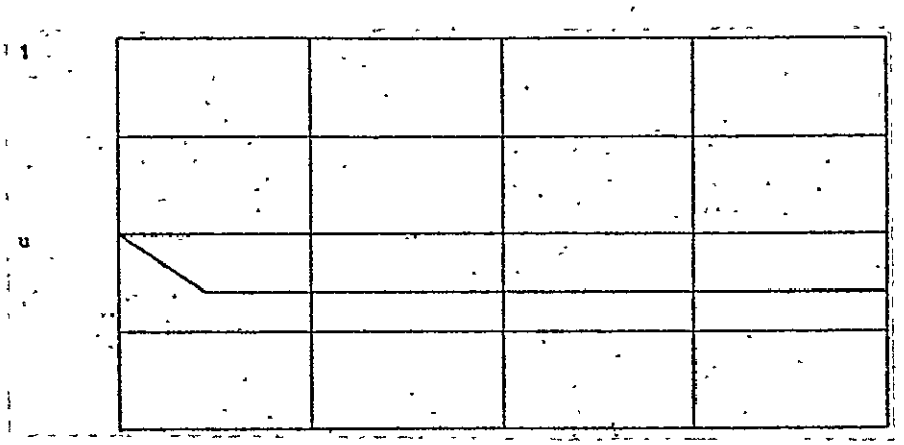

Figure 82. Control variable.

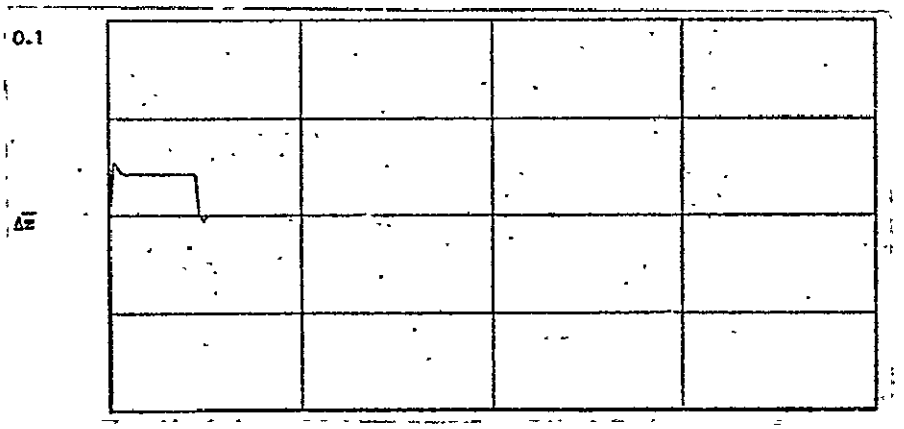

Figure 83. Relative deflection.

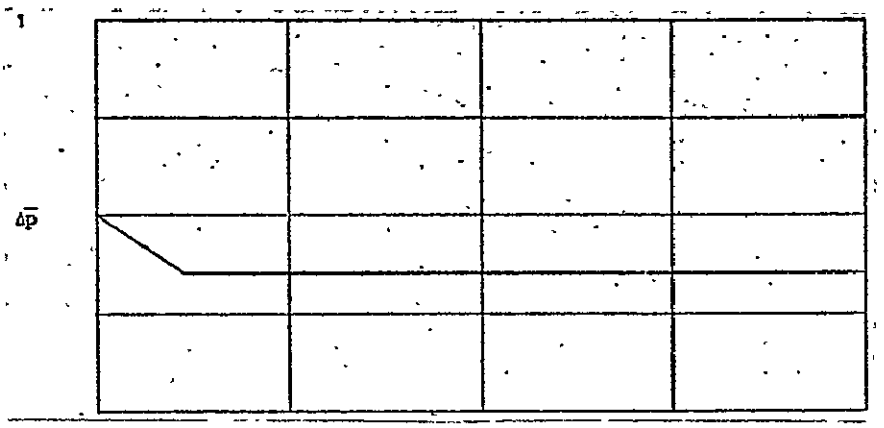

/58

Figure 84. Differential pressure of actuator.

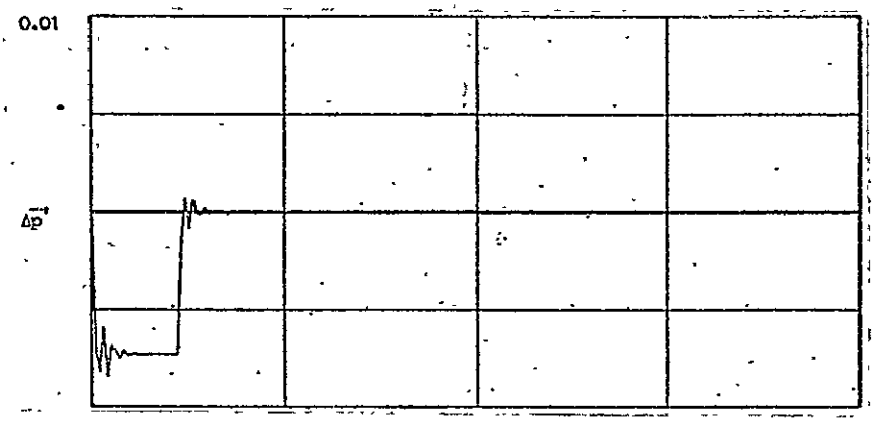

Figure 85. Derivative of differential pressure.

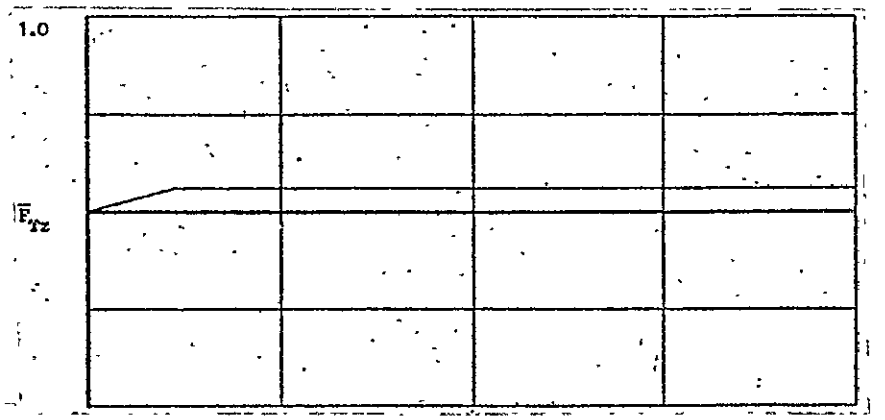

Figure 86. Isolation force.

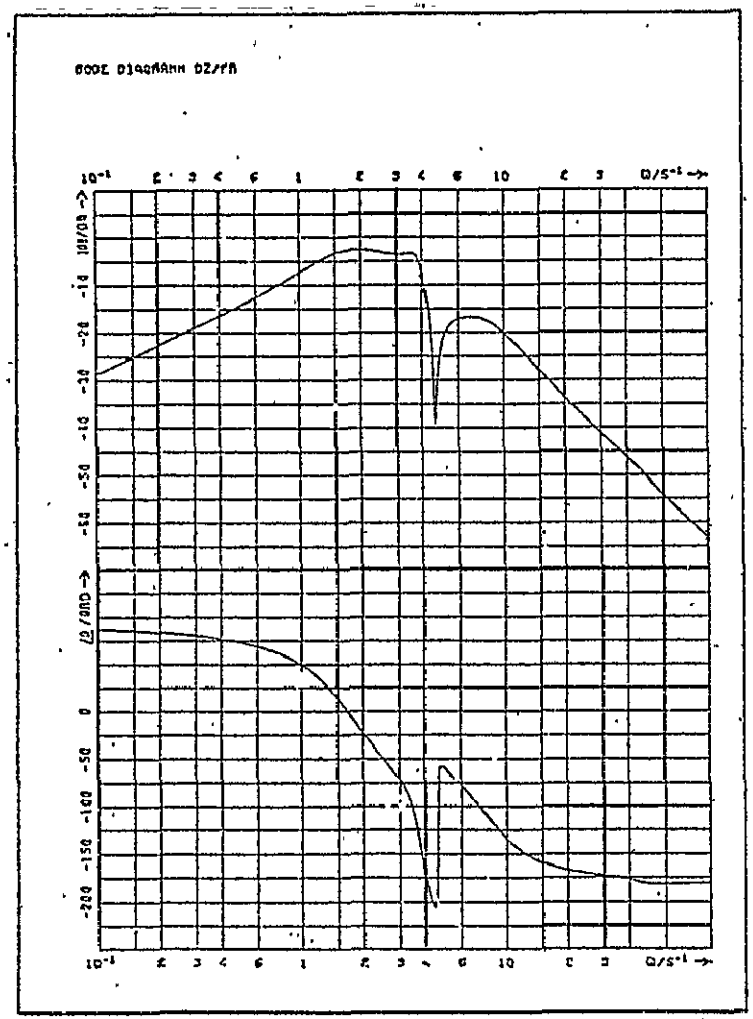

Figure 87. Bode diagram of perturbation function of relative deflection.

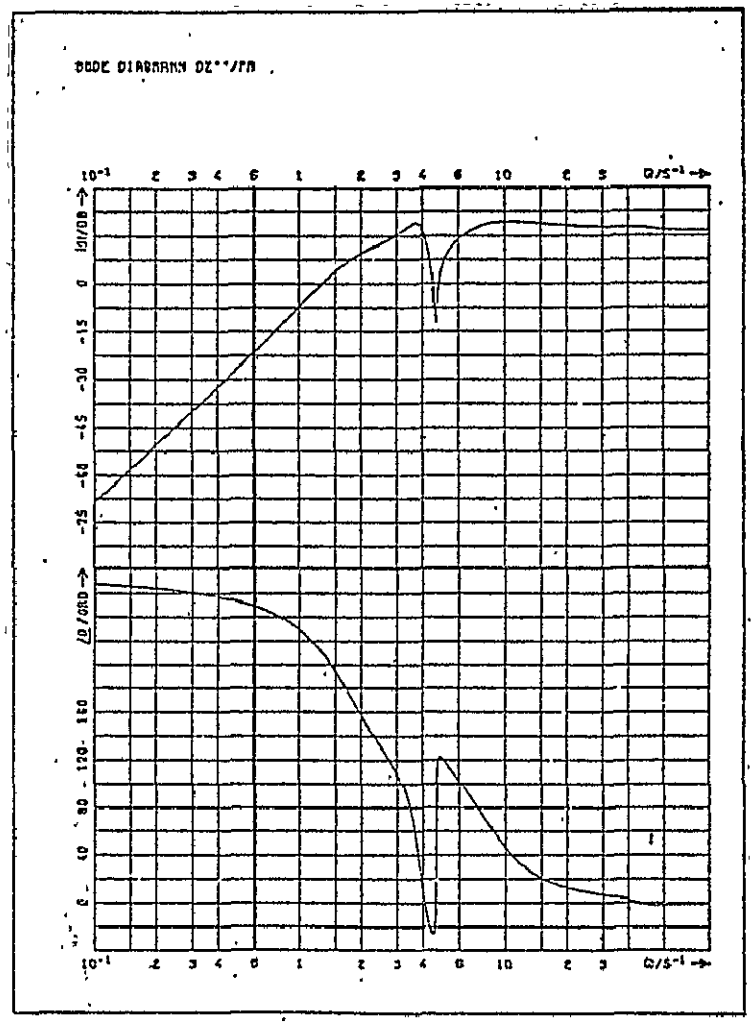

Figure 88. Bode diagram of perturbation function of relative acceleration.

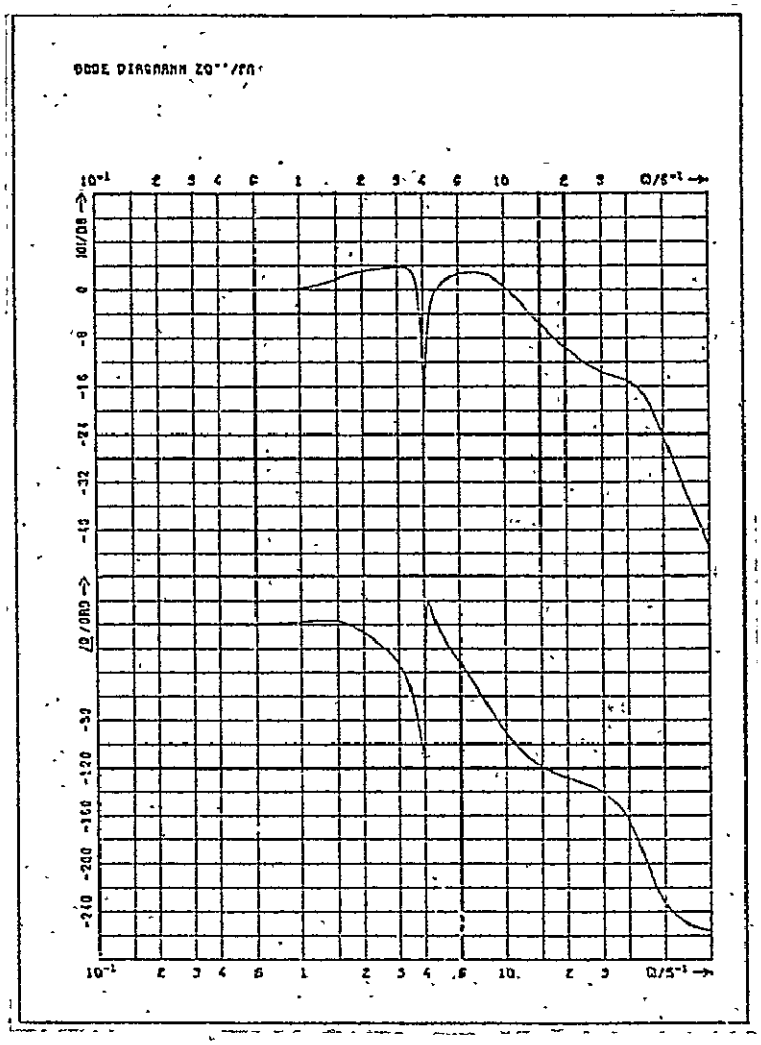

Figure 89. Bode diagram of perturbation function of airframe acceleration.

/ 60

ORIGINAL PAGE IS
OF POOR QUALITY